

Table of Contents

- 1. Materials**
- 2. Measurements**
- 3. Syntheses and characterization of host compounds, H1-H4**
- 4. ^1H NMR studies**
- 5. Binding studies**
- 6. X-ray crystallographic analysis**
- 7. Characterization data of new compounds, H3-H4**
- 8. References**

Supporting Information

1. Materials

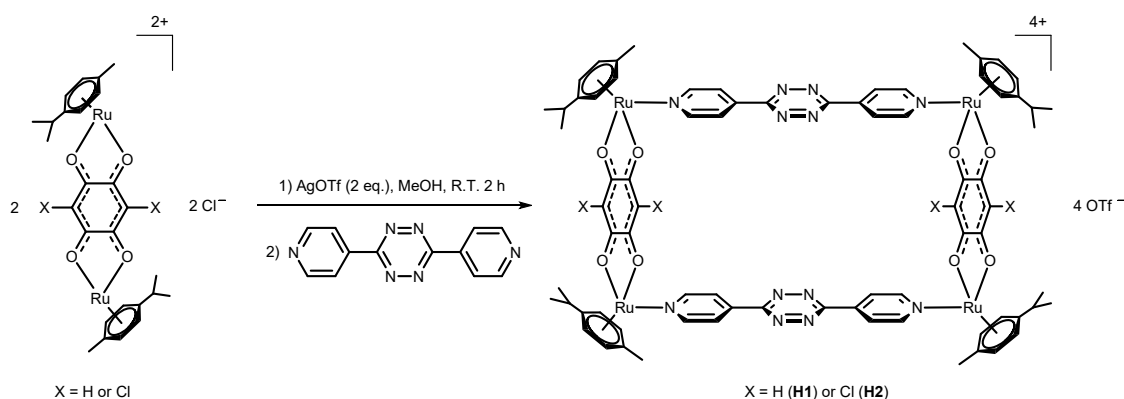
All reagent-grade chemicals and organic solvents were purchased from Sigma-Aldrich, Alfa Aesar and Acros, and used without further purifications. $[\text{Ru}_2(p\text{-cymene})_2(\mu\text{-Cl})_2\text{Cl}_2]^{\text{S1}}$, $[\text{Ru}_2(p\text{-cymene})_2(\text{dobq})\text{Cl}_2]^{\text{S2}}$ (dobp= 2,5-dihydroxy-1,4-benzoquinone), $[\text{Ru}_2(p\text{-cymene})_2(\text{dcbq})\text{Cl}_2]^{\text{S2}}$ (dcbp= 2,5-dichloro-3,6-dihydroxy-1,4-benzoquinone), and 3,6-di(4-pyridyl)-s-tetrazine^{S3,S4} were synthesized based on literature methods.

2. Measurements

NMR spectra were measured by using Bruker Avance II DRX 400 and Avance III HD 300 instruments. Chemical shifts were reported using residual protonated solvent peaks (for ^1H NMR spectra, acetone- d_6 2.05 ppm; CDCl_3 7.26 ppm; DMSO- d_6 2.50 ppm). Fluorescence spectra were measured by Hitachi F-4500 fluorescence spectrophotometer. 3-D crystal structure of **H2** \supset perylene was obtained by a Bruker D8 Venture diffractometer. ESI mass spectra were measured by Agilent 6230 TOF LC/MS. The Elemental Analysis measurements were obtained from *the Organic Chemistry Research Centre at Sogang University*.

3. Syntheses and characterization of host compounds, H1-H4

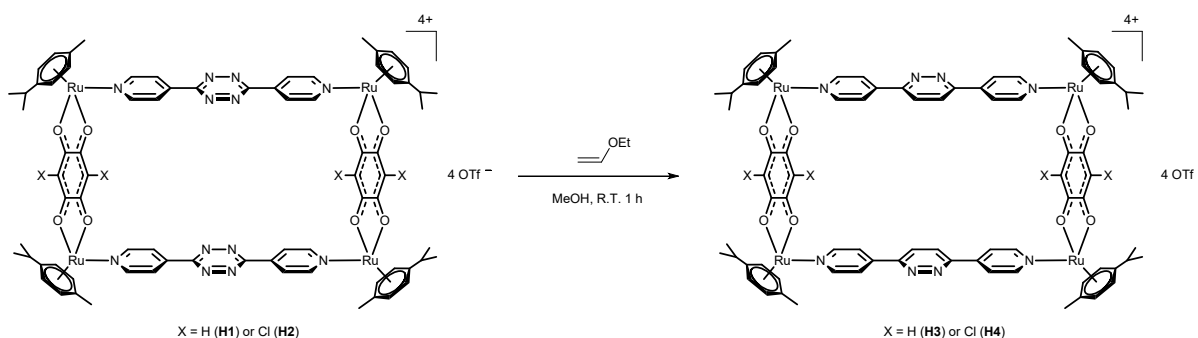
3.1 Synthesis of H1^{S5} and H2^{S5}



$[\text{Ru}_4(p\text{-cymene})_4(\text{dobp})_2(\text{bptz})_2][\text{OTf}]_4$ (**H1**) : $[\text{Ru}_2(p\text{-cymene})_2(\text{dobq})\text{Cl}_2]$ (100 mg, 0.15 mmol), and AgOTf (76 mg, 0.30 mmol) were stirred in methanol (30 mL) for 2 h at room temperature. Then, 3,6-di(4-pyridyl)-s-tetrazine (35 mg, 0.15 mmol) was added and the mixture was stirred for 3 h at room temperature. The solution was filtered over celite, and then the solvent was removed under vacuum. The solid was washed with dichloromethane(DCM) to yield **H1** (136 mg, 81%). ^1H NMR (400 MHz, acetone- d_6 , 25 °C, ppm): δ = 8.77 (d, J = 6.72 Hz, 8H), 8.53 (d, J = 6.72 Hz, 8H), 6.25 (d, J = 6.36 Hz, 8H), 6.06 (d, J = 6.36 Hz, 8H), 5.87 (s, 4H), 3.00 (sept, J = 6.97 Hz, 4H), 2.30 (s, 12H), 1.41 (d, J = 6.92 Hz, 24H). Elemental analysis calcd (%) for $\text{C}_{80}\text{H}_{76}\text{F}_{12}\text{N}_{12}\text{O}_{20}\text{Ru}_4\text{S}_4$: C 42.03, H 3.35, N 7.35; found C 41.96, H 3.23, N 7.21.

$[\text{Ru}_4(p\text{-cymene})_4(\text{dcbq})_2(\text{bptz})_2][\text{OTf}]_4$ (**H2**) : $[\text{Ru}_2(p\text{-cymene})_2(\text{dcbq})\text{Cl}_2]$ (100 mg, 0.13 mmol), and AgOTf (69 mg, 0.27 mmol) were stirred in methanol (30 mL) for 2 h at room temperature. Then, 3,6-di(4-pyridyl)-s-tetrazine (31 mg, 0.13 mmol) was added and the mixture was stirred for 3 h at room temperature. The solution was filtered over celite, and then the solvent was removed under vacuum. The solid was washed with DCM to yield **H2** (144 mg, 89%). ^1H NMR (400 MHz, acetone- d_6 , 25 °C, ppm): δ = 8.77 (d, J = 6.68 Hz, 8H), 8.56 (d, J = 6.68 Hz, 8H), 6.33 (d, J = 6.32 Hz, 8H), 6.16 (d, J = 6.32 Hz, 8H), 3.08 (sept, J = 7.04 Hz, 4H), 2.40 (s, 12H), 1.48 (d, J = 6.92 Hz, 24H). Elemental analysis calcd (%) for $\text{C}_{80}\text{H}_{72}\text{Cl}_4\text{F}_{12}\text{N}_{12}\text{O}_{20}\text{Ru}_4\text{S}_4$: C 39.64, H 2.99, N 6.93; found C 39.65, H 2.89, N 6.87.

3.2 Synthesis of H3 and H4 (IEDDA reaction)



$[\text{Ru}_4(p\text{-cymene})_4(\text{dobp})_2(\text{bppz})_2][\text{OTf}]_4$ (**H3**) (bppz: 3,6-di-(4-pyridyl)-pyridazine) : **H1** (100 mg, 0.044 mmol) and ethyl vinyl ether (1 mL, 10 mmol) were stirred in methanol (15 mL) for 1 h at room temperature. The solvent was removed under vacuum (95 mg, 95%). ^1H NMR (400 MHz, acetone- d_6 , 25 °C, ppm): δ = 8.63 (d, J = 5.7 Hz, 8H), 8.48 (s, 4H), 8.35 (d, J = 6.0 Hz, 8H), 6.24 (d, J = 6.1 Hz, 8H), 6.04 (d, J = 6.0 Hz, 8H), 5.88 (s, 4H), 3.00 (sept, J = 6.8 Hz, 4H), 2.29 (s, 12H), 1.41 (d, J = 6.9 Hz, 24H). ^{13}C NMR (100 MHz, acetone- d_6 , 25 °C, ppm): δ = 184.35, 154.95, 153.95, 145.37, 126.03, 123.20, 119.79, 103.78, 101.78, 99.23, 83.85, 82.21, 31.24, 21.65, 17.30. ESI-TOF-MS: m/z 611.7021 $[\text{M}-3\text{OTf}]^{3+}$, 992.0696 $[\text{M}-2\text{OTf}]^{2+}$, 2133.0533 $[\text{M}-\text{OTf}]^+$. Elemental analysis calcd (%) for $\text{C}_{84}\text{H}_{80}\text{F}_{12}\text{N}_8\text{O}_{20}\text{Ru}_4\text{S}_4$: C 44.21, H 3.53, N 4.91, S 5.62; found C 44.24, H 3.61, N 4.91, S 5.60.

$[\text{Ru}_4(p\text{-cymene})_4(\text{dcbq})_2(\text{bppz})_2][\text{OTf}]_4$ (**H4**) : **H2** (100 mg, 0.044 mmol) and ethyl vinyl ether (1 mL, 10 mmol) were stirred in methanol (15 mL) for 1 h at room temperature. The solvent was removed under vacuum (95 mg, 95%). ^1H NMR (400 MHz, acetone- d_6 , 25 °C, ppm): δ = 8.61 (d, J = 6.68 Hz, 8H), 8.51 (s, 4H), 8.36 (d, J = 6.68 Hz, 8H), 6.31 (d, J = 6.44 Hz, 8H), 6.13 (d, J = 6.28 Hz, 8H), 3.05 (sept, J = 6.93 Hz, 4H), 2.37 (s, 12H), 1.46 (d, J = 6.88 Hz, 24H). ^{13}C NMR (100 MHz, acetone- d_6 , 25 °C, ppm): δ = 177.89, 155.01, 153.86, 145.44, 126.17, 123.34, 119.77, 106.18, 104.02, 99.00, 83.83, 82.88, 31.34, 21.57, 17.35. ESI-TOF-MS: m/z 657.6740 $[\text{M}-3\text{OTf}]^{3+}$, 1060.9532 $[\text{M}-2\text{OTf}]^{2+}$, 2270.9527 $[\text{M}-\text{OTf}]^+$. Elemental analysis calcd (%) for $\text{C}_{84}\text{H}_{76}\text{Cl}_4\text{F}_{12}\text{N}_8\text{O}_{20}\text{Ru}_4\text{S}_4$: C 41.69, H 3.17, N 4.63; found C 41.72, H 3.04, N 4.76.

4. ^1H NMR studies

4.1. ^1H NMR spectral changes of H1 on each guest

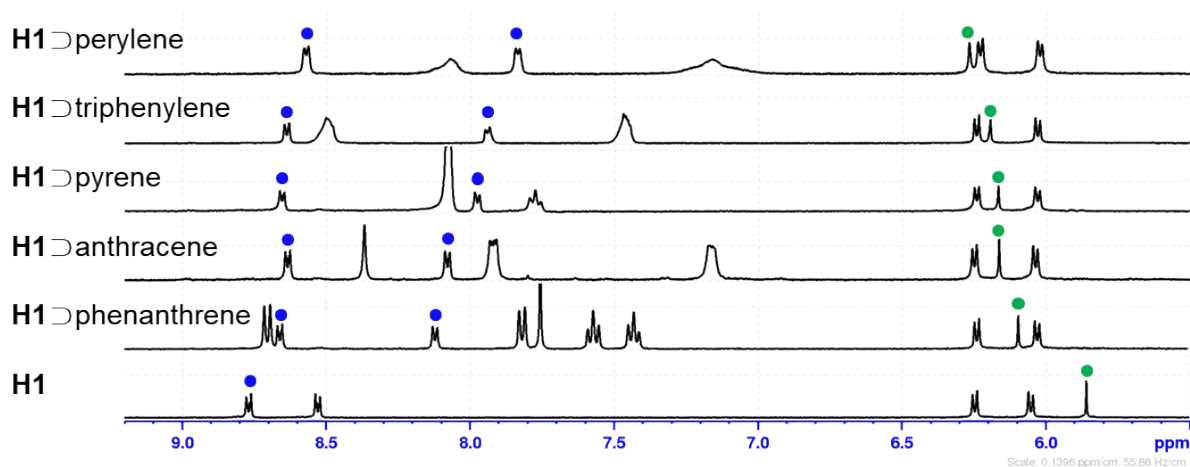


Figure S1. Partial ^1H NMR spectra (400 MHz, 25 °C) of H1 with the presence of each guest in acetone- d_6 . Aromatic CH signals for bptz in H1 depicted as blue dots and CH signals for benzoquinone as green dots.

4.2. ^1H NMR spectral changes of H2 on each guest

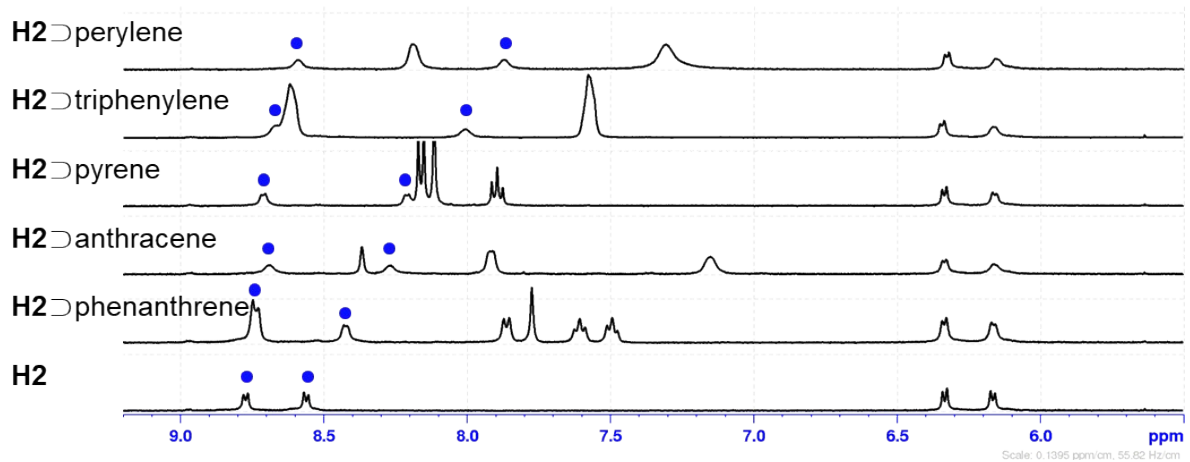


Figure S2. Partial ^1H NMR spectra (400 MHz, 25 °C) of H2 with the presence of each guest in acetone- d_6 . Aromatic CH signals for bptz in H2 depicted as blue dots.

4.3. ¹H NMR spectral changes of H3 on each guest

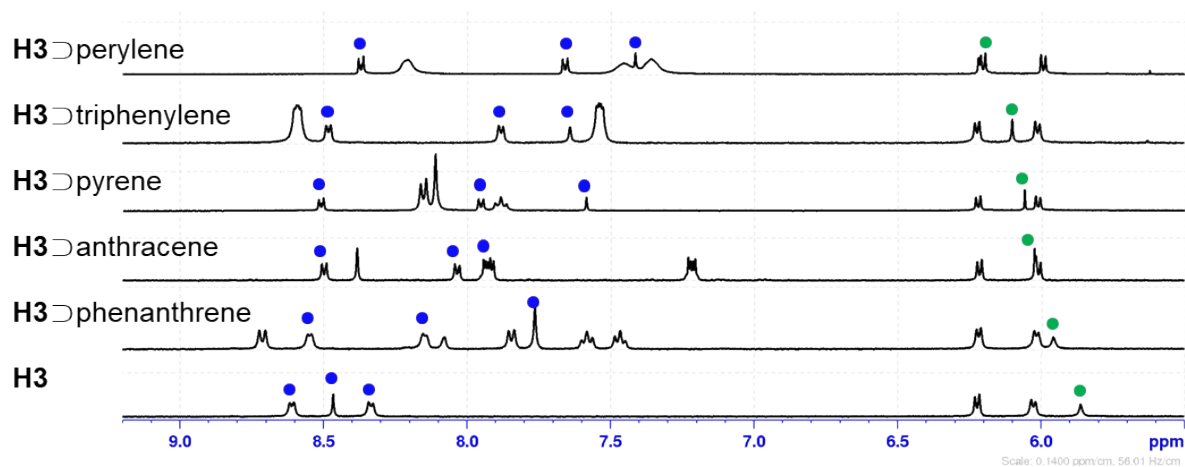


Figure S3. Partial ¹H NMR spectra (400 MHz, 25 °C) of **H3** with the presence of each guest in acetone-*d*₆. Aromatic CH signals for bppz in **H3** depicted as blue dots and CH signals for benzoquinone as green dots.

4.4. ¹H NMR spectral changes of H4 on each guest

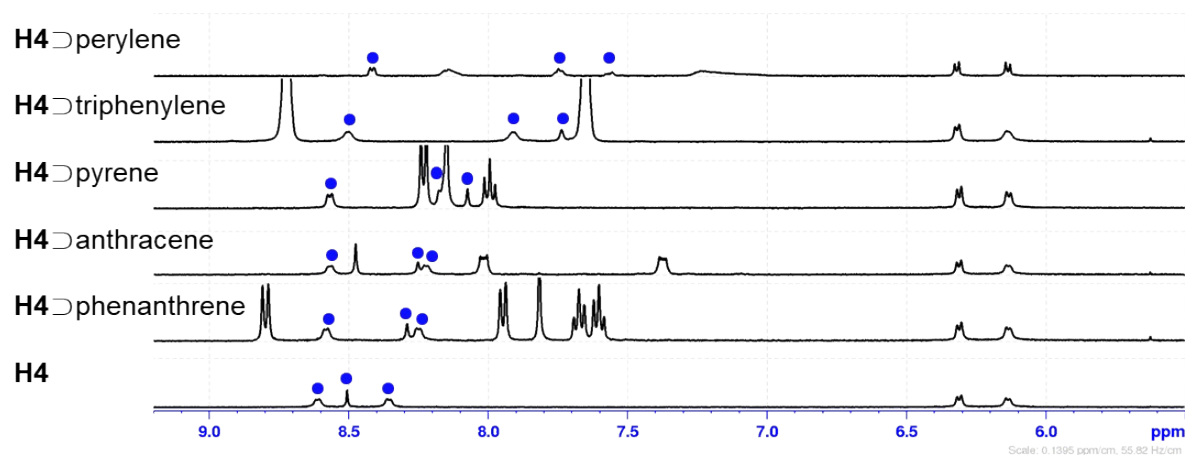


Figure S4. Partial ¹H NMR spectra (400 MHz, 25 °C) of **H4** with the presence of each guest in acetone-*d*₆. Aromatic CH signals for bppz in **H4** depicted as blue dots.

4.5. ^1H NMR spectral changes of the IEDDA reaction in H2

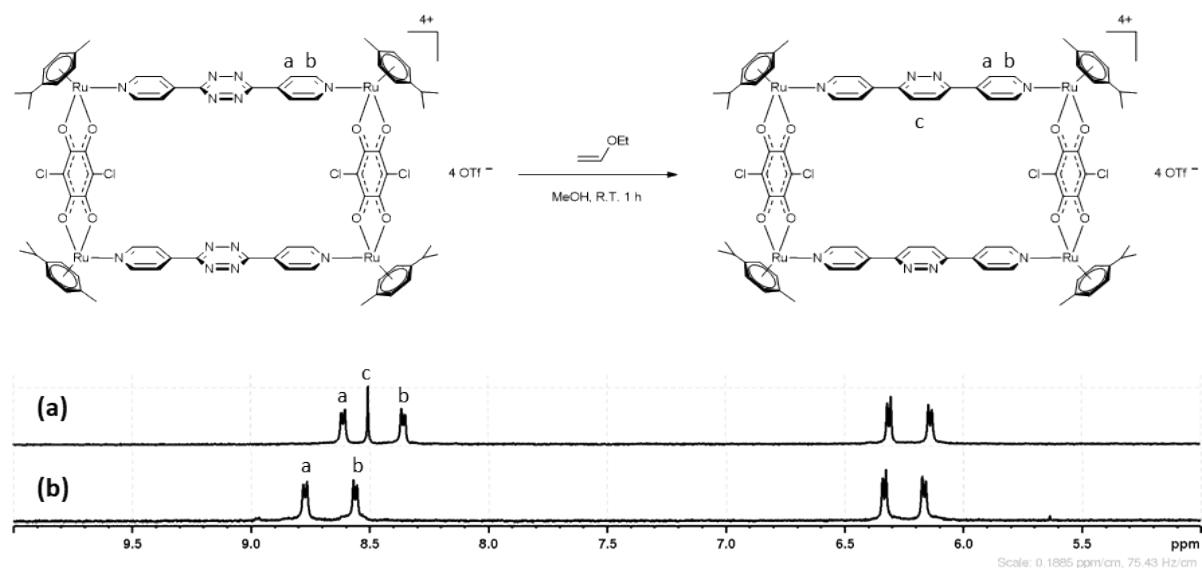


Figure S5. Partial ^1H NMR spectra (400 MHz, 25 °C) of (a) **H4** and (b) **H2** after the IEDDA reaction.

5. Binding studies

5.1 General

5.1.1 ¹H NMR titration experiment

Stock solutions of the host compounds were prepared in acetone-*d*₆ at 25 °C. Using this solution, stock solutions of the guest compounds were prepared in 5 to 10-fold concentrated than the host stock solutions. A 500 μL of the host stock solution was transferred to a NMR tube, and the initial spectrum was taken. After each addition of aliquots of the guest stock solution, the spectrum was taken. Each titration curve was obtained by plotting the chemical shift changes against the equivalents of the guest compounds. Association constant (*K*_a) values were calculated by using *bindfit* software.^{S6}

5.1.2 Fluorescence titration experiment

Stock solutions of the host compounds (2.0×10^{-6} M) were prepared in acetone. Using this solution, guest stock solution of perylene (2.0×10^{-4} M) were prepared. A 1.80 mL of the host solution was transferred to the cuvette and the initial spectrum was recorded. Aliquots of the perylene solution were added to the cuvette containing each host solution and the spectra were recorded. Each titration curve was obtained by plotting the chemical shift changes against the equivalents of perylene. Association constant (*K*_a) values were calculated by using *bindfit* software.^{S6}

5.2 Binding study of H1

5.2.1 H1 ⊃ phenanthrene

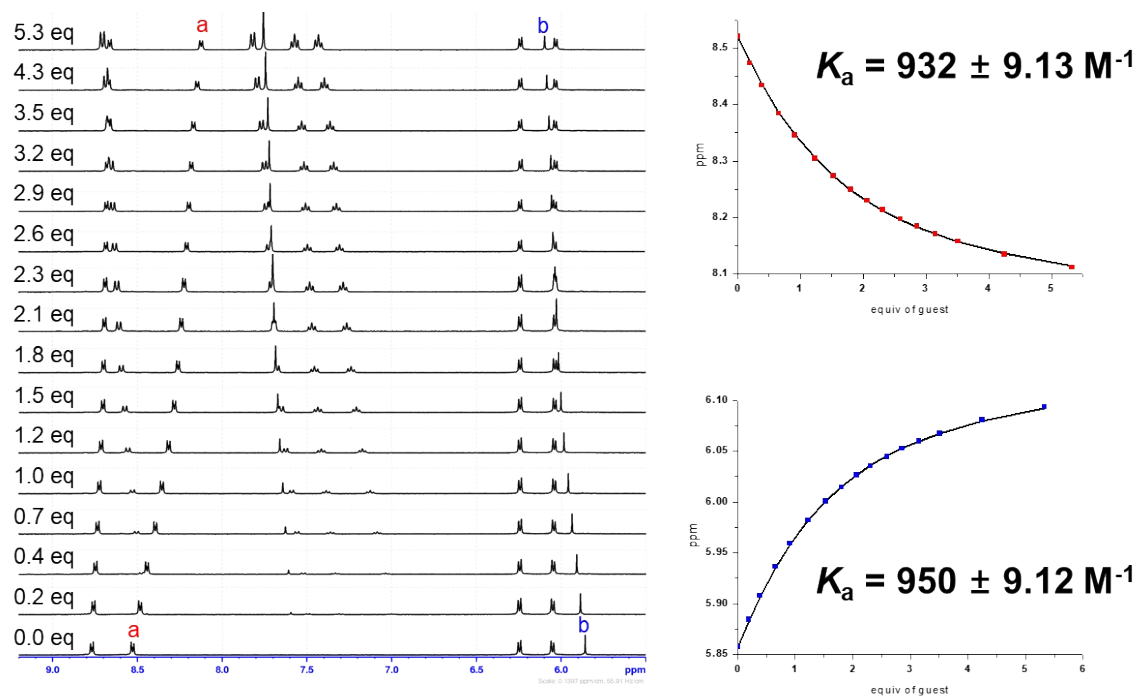


Figure S6. Partial ^1H NMR spectra of H1 (1.00×10^{-3} M) with the addition of phenanthrene (1.00×10^{-2} M) in acetone- d_6 . The experimental (dots) and theoretical fitting (line) curves of ^1H NMR signals are shown right. A mean value (\pm standard deviation) of K_a is $(9.41 \pm 0.127) \times 10^2 \text{ M}^{-1}$.

5.2.2 H1 ⊃ anthracene

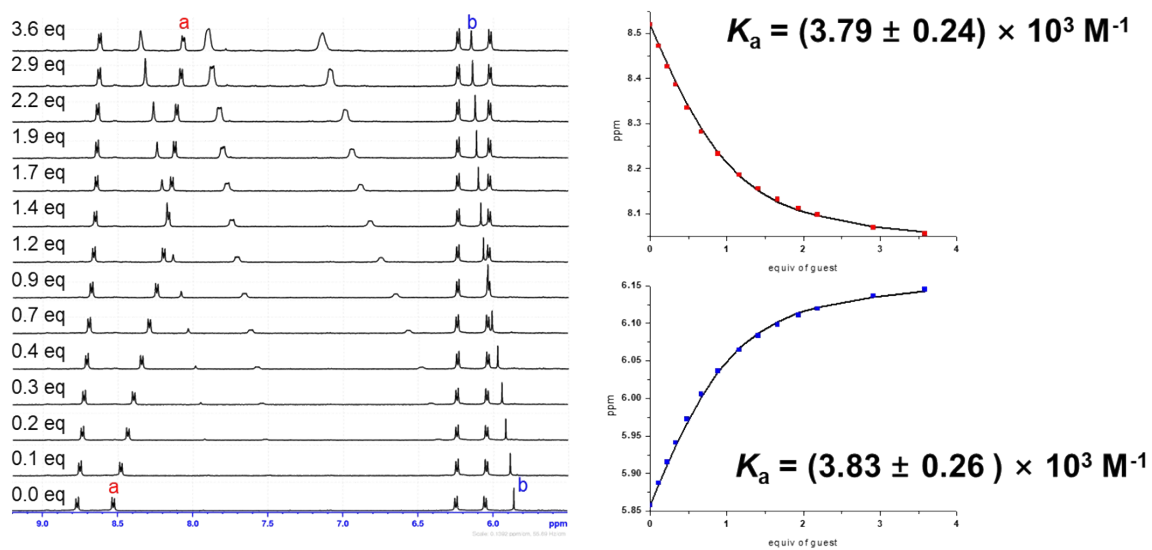


Figure S7. Partial ¹H NMR spectra of **H1** (1.10×10^{-3} M) with the addition of anthracene (6.4×10^{-3} M) in acetone-*d*₆. The experimental (dots) and theoretical fitting (line) curves of ¹H NMR signals are shown right. A mean value (\pm standard deviation) of K_a is $(3.811 \pm 0.0318) \times 10^3 \text{ M}^{-1}$.

5.2.3 H1 ⊃ pyrene

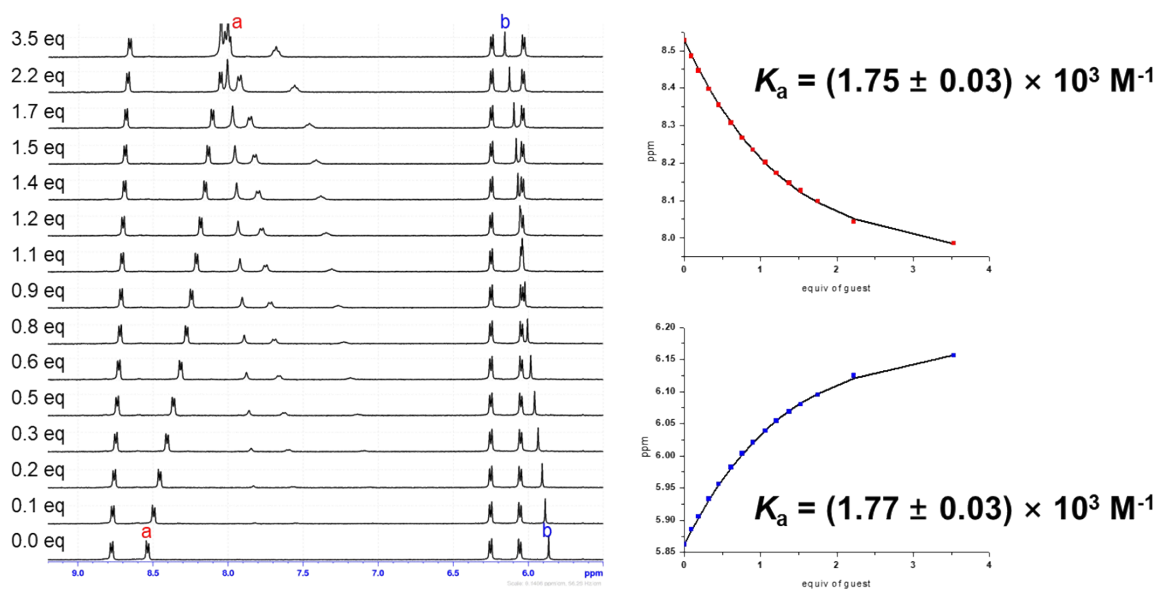


Figure S8. Partial ¹H NMR spectra of H1 (1.00×10^{-3} M) with the addition of pyrene (5.00×10^{-3} M) in acetone-*d*₆. The experimental (dots) and theoretical fitting (line) curves of ¹H NMR signals are shown right. A mean value (\pm standard deviation) of K_a is $(1.759 \pm 0.0198) \times 10^3 \text{ M}^{-1}$.

5.2.4 H1 ⊃ triphenylene

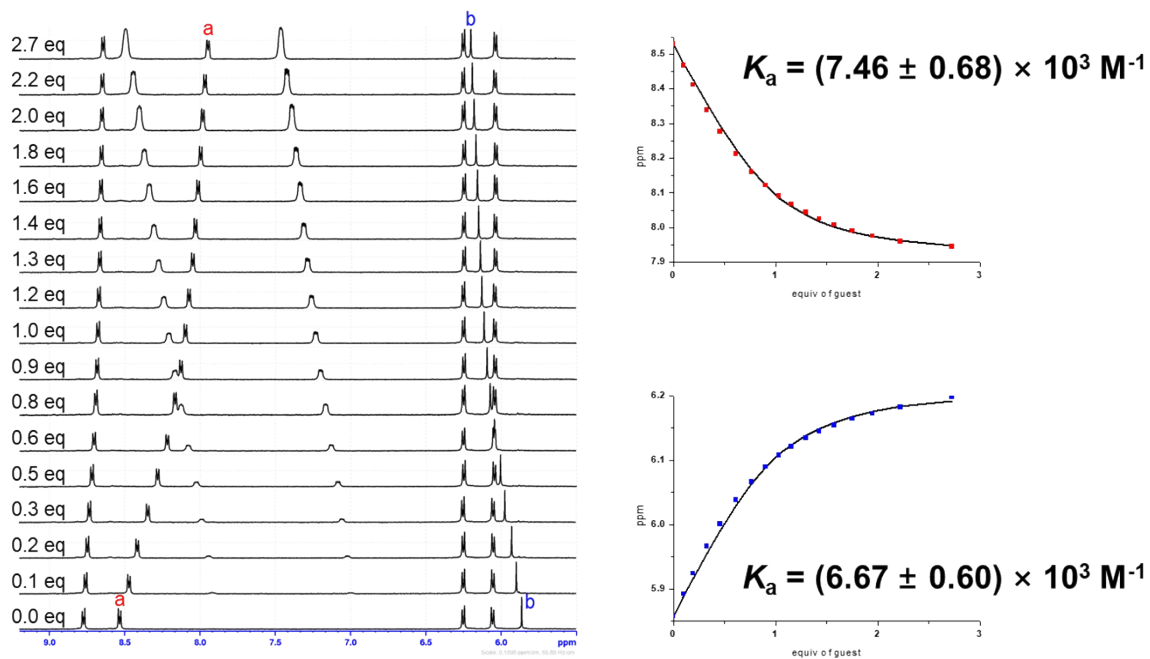


Figure S9. Partial ^1H NMR spectra of H1 (1.00×10^{-3} M) with the addition of triphenylene (5.00×10^{-3} M) in acetone- d_6 . The experimental (dots) and theoretical fitting (line) curves of ^1H NMR signals are shown right. A mean value (\pm standard deviation) of K_a is $(7.062 \pm 0.5614) \times 10^3 \text{ M}^{-1}$.

5.2.5 H1⊃perylene

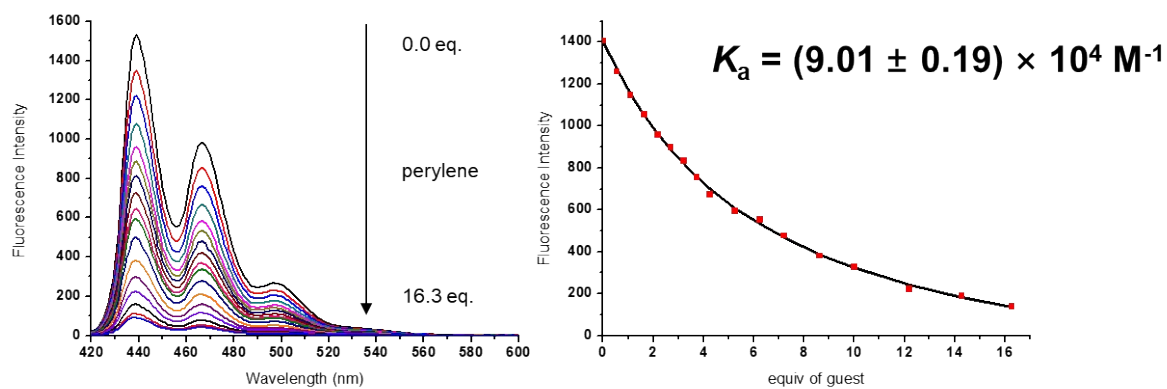


Figure S10. Fluorescence emission spectra (λ_{max} : 439 nm) of **H1** (2.00×10^{-6} M) with the addition of perylene in acetone, and fitting curve at 439 nm are shown right.

5.3 Binding study of H2

5.3.1 H2 ⊃ phenanthrene

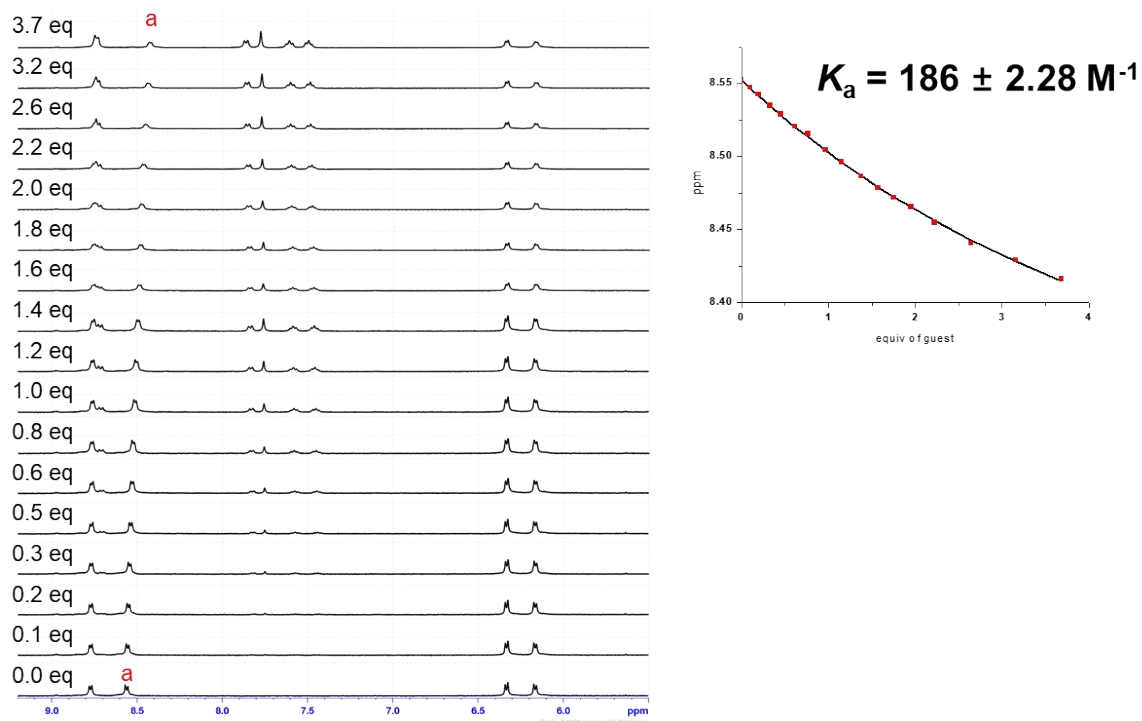


Figure S11. Partial ¹H NMR spectra of H2 (1.00 × 10⁻³ M) with the addition of phenanthrene (5.00 × 10⁻³ M) in acetone-*d*₆. The experimental (dots) and theoretical fitting (line) curves of ¹H NMR signals are shown right.

5.3.2 H2⊂anthracene

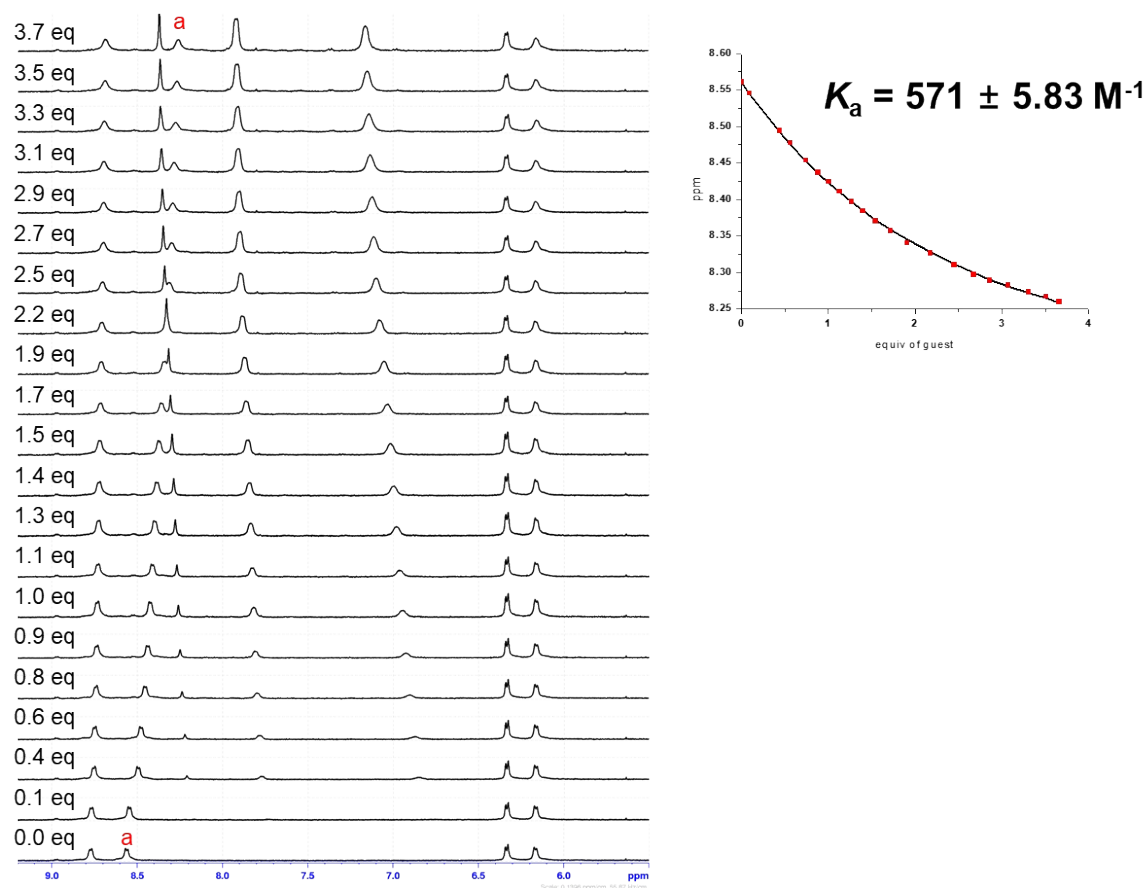


Figure S12. Partial ¹H NMR spectra of H2 (1.00 × 10⁻³ M) with the addition of anthracene (4.90 × 10⁻³ M) in acetone-*d*₆. The experimental (dots) and theoretical fitting (line) curves of ¹H NMR signals are shown right.

5.3.3 H2⊃pyrene

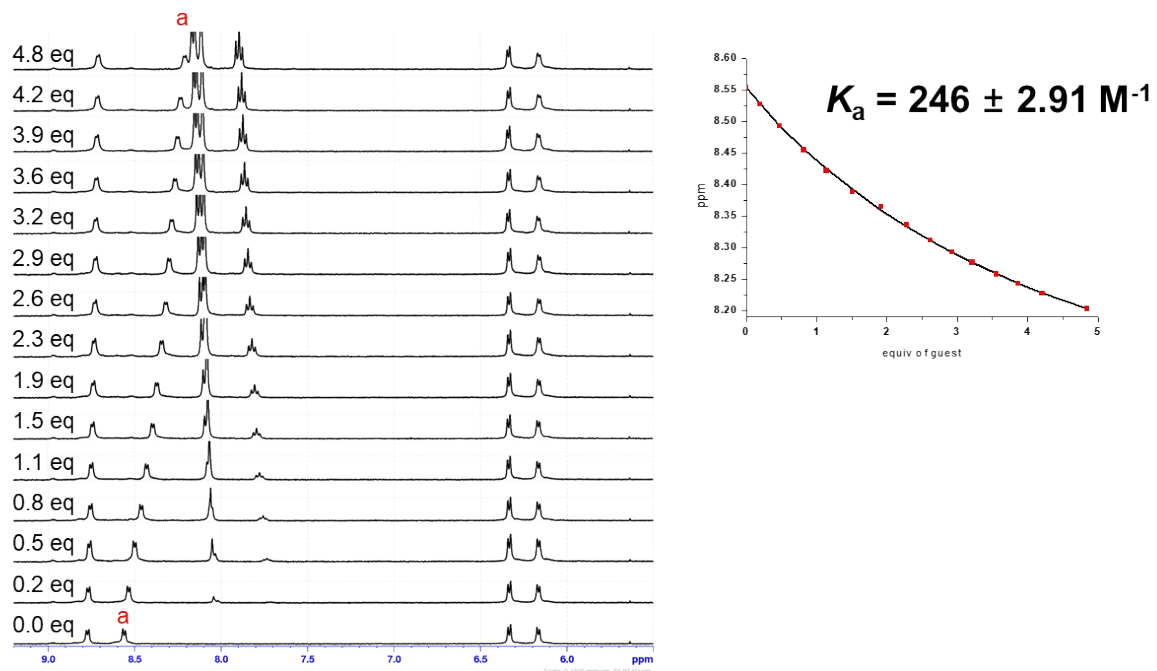


Figure S13. Partial ¹H NMR spectra of H2 (9.9 × 10⁻⁴ M) with the addition of pyrene (9.8 × 10⁻³ M) in acetone-*d*₆. The experimental (dots) and theoretical fitting (line) curves of ¹H NMR signals are shown right.

5.3.4 H2 ⊂ triphenylene

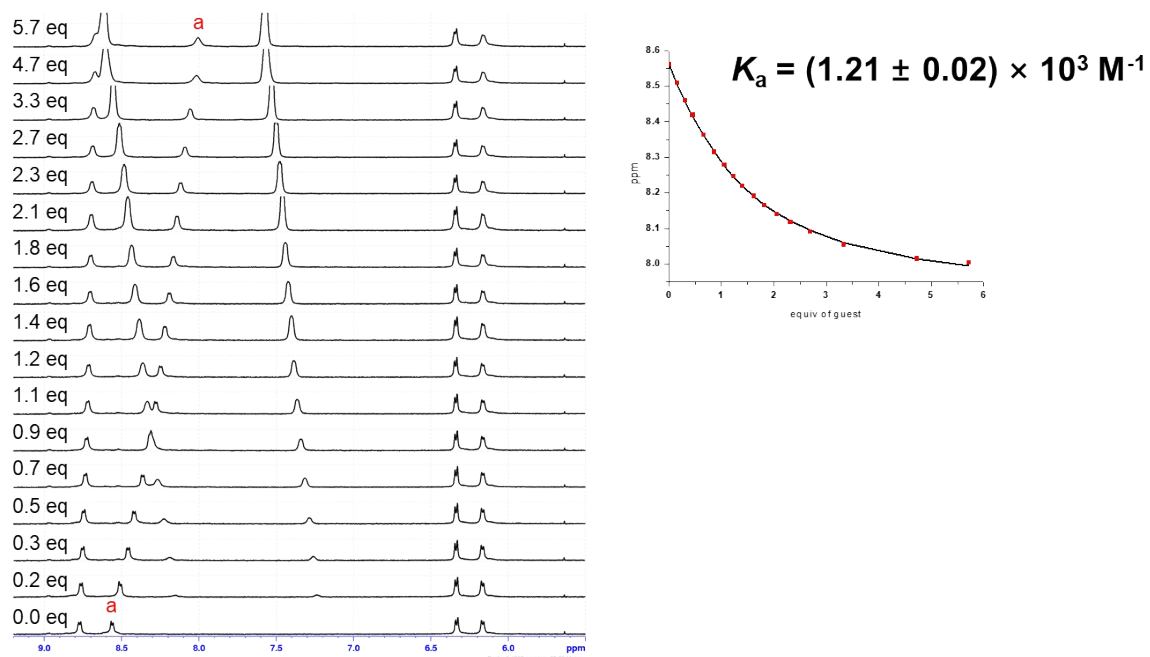


Figure S14. Partial ^1H NMR spectra of **H2** (1.00×10^{-3} M) with the addition of triphenylene (8.10×10^{-3} M) in acetone- d_6 . The experimental (dots) and theoretical fitting (line) curves of ^1H NMR signals are shown right.

5.3.5 H2⊃perylene

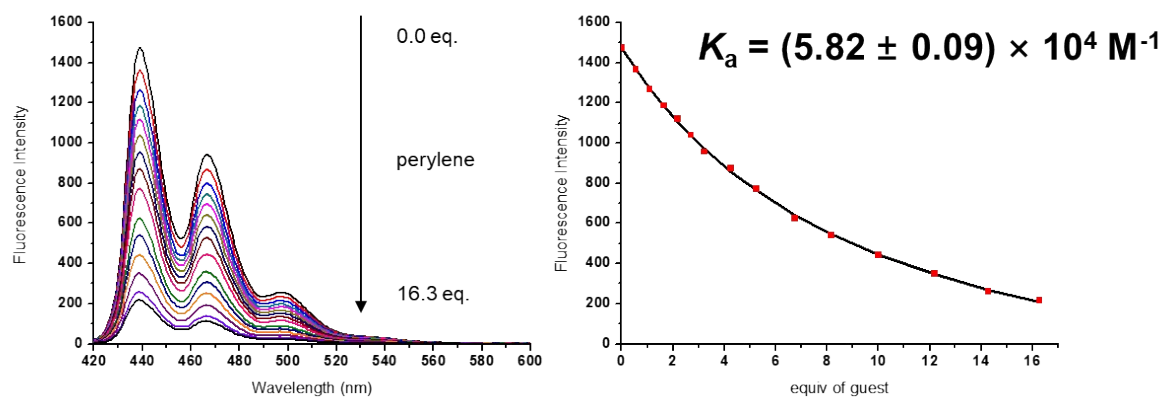


Figure S15. Fluorescence emission spectra (λ_{max} : 439 nm) of **H2** (2.00×10^{-6} M) with the addition of perylene in acetone, and fitting curve at 439 nm are shown right.

5.4 Binding study of H3

5.4.1 H3 ⊃ phenanthrene

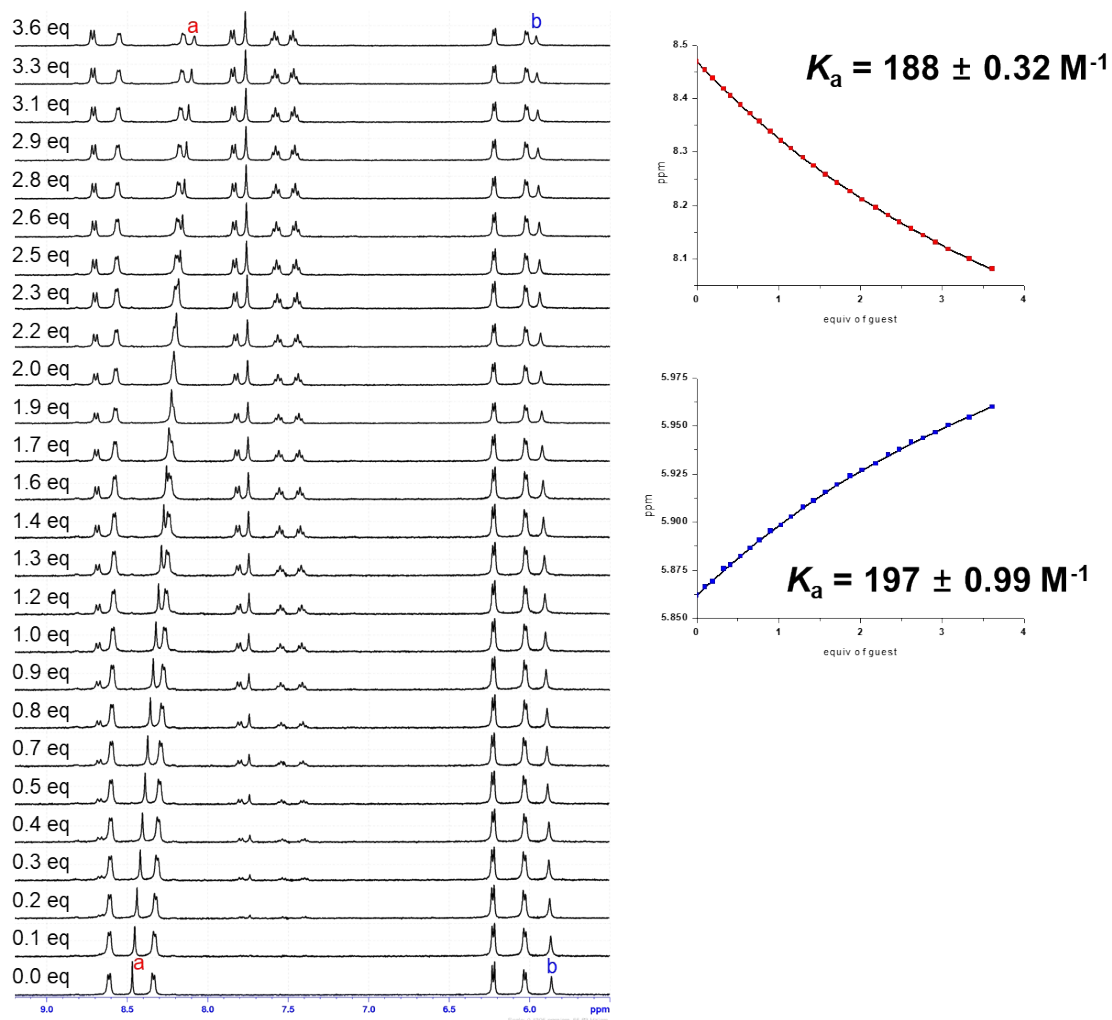


Figure S16. Partial ¹H NMR spectra of H3 (1.00×10^{-3} M) with the addition of phenanthrene (1.00×10^{-2} M) in acetone-d₆. The experimental (dots) and theoretical fitting (line) curves of ¹H NMR signals are shown right. A mean value (\pm standard deviation) of K_a is $(1.93 \pm 0.064) \times 10^2 \text{ M}^{-1}$.

5.4.2 H3⊂anthracene

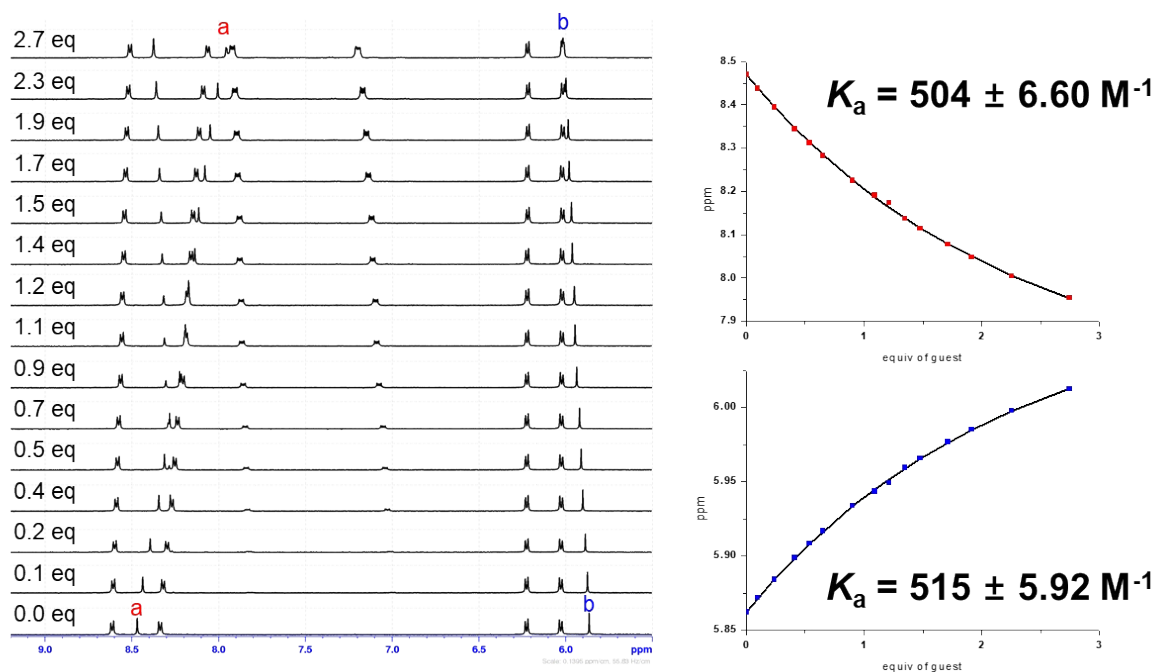


Figure S17. Partial ^1H NMR spectra of H3 (1.00×10^{-3} M) with the addition of anthracene (5.00×10^{-3} M) in acetone- d_6 . The experimental (dots) and theoretical fitting (line) curves of ^1H NMR signals are shown right. A mean value (\pm standard deviation) of K_a is $(5.10 \pm 0.078) \times 10^2 \text{ M}^{-1}$.

5.4.3 H3⊂pyrene

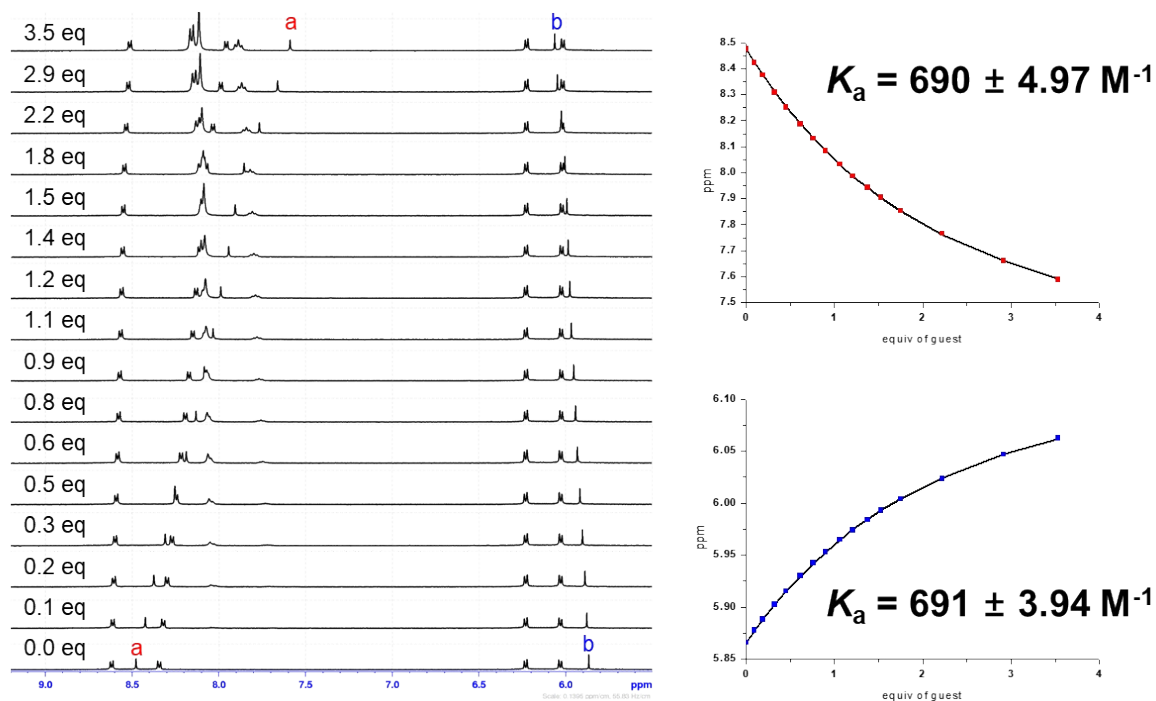


Figure S18. Partial ¹H NMR spectra of H3 ($1.00 \times 10^{-3} \text{ M}$) with the addition of pyrene ($5.00 \times 10^{-3} \text{ M}$) in acetone-*d*₆. The experimental (dots) and theoretical fitting (line) curves of ¹H NMR signals are shown right. A mean value (\pm standard deviation) of K_a is $(6.90 \pm 0.007) \times 10^2 \text{ M}^{-1}$.

5.4.4 H3 ⊂ triphenylene

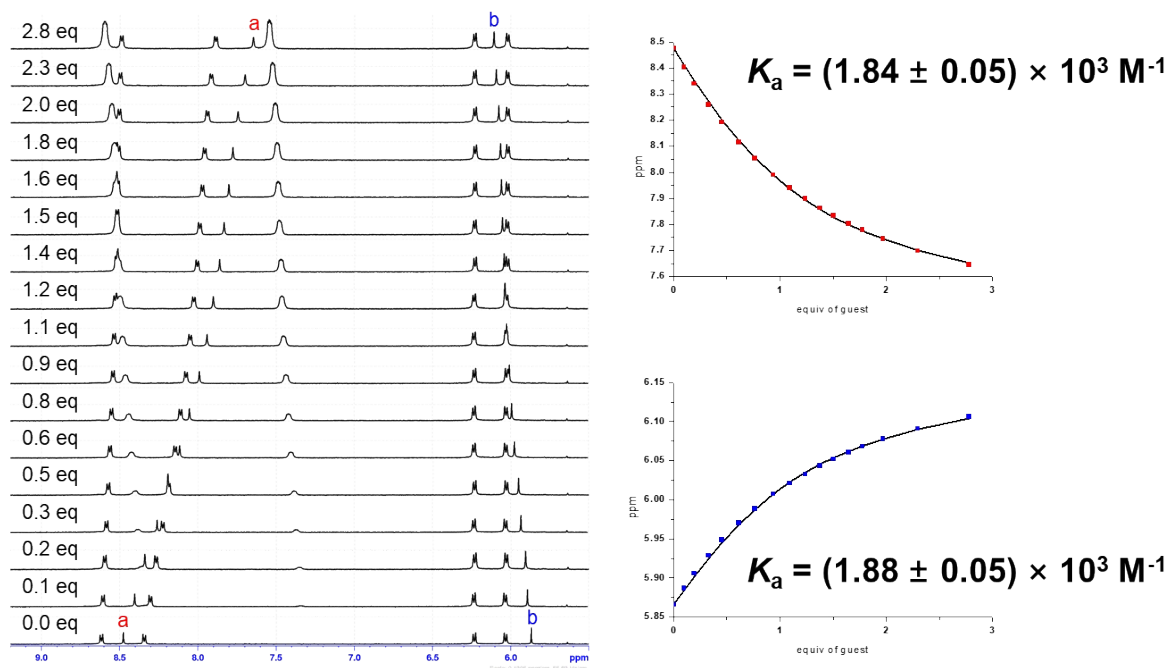


Figure S19. Partial ¹H NMR spectra of H3 (1.00 × 10⁻³ M) with the addition of triphenylene (5.00 × 10⁻³ M) in acetone-*d*₆. The experimental (dots) and theoretical fitting (line) curves of ¹H NMR signals are shown right. A mean value (± standard deviation) of K_a is (1.861 ± 0.0297) × 10³ M⁻¹.

5.4.5 H3⊂perylene

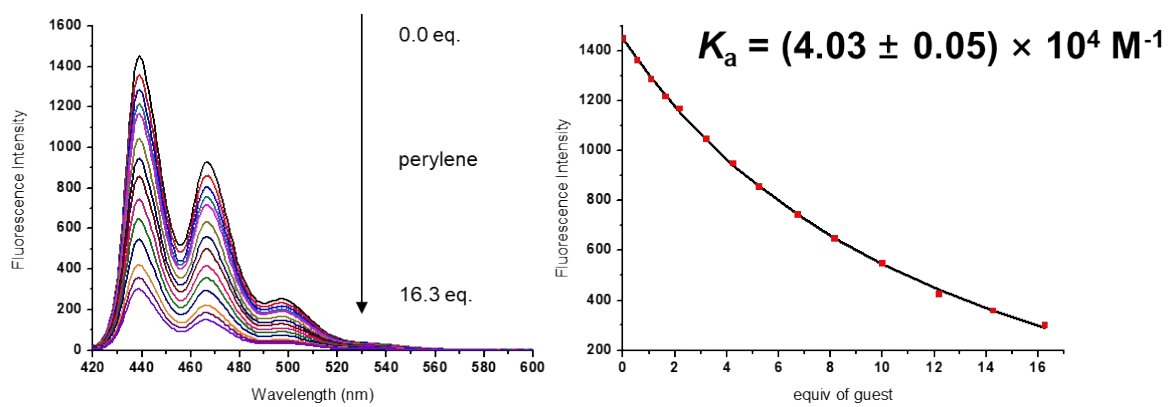


Figure S20. Fluorescence emission spectra (λ_{max} : 439 nm) of **H3** (2.00×10^{-6} M) with the addition of perylene in acetone, and fitting curve at 439 nm are shown right.

5.5 Binding study of H4

5.5.1 H4 + phenanthrene

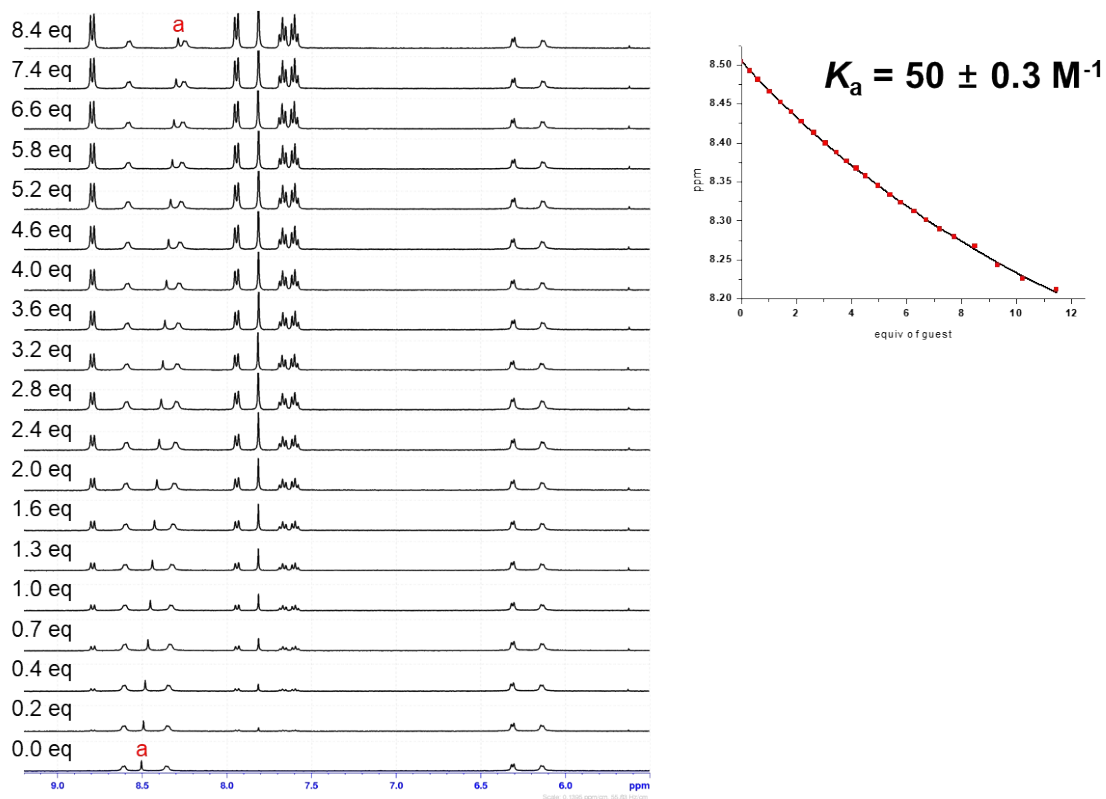


Figure S21. Partial ¹H NMR spectra of H4 (1.00 × 10⁻³ M) with the addition of phenanthrene (1.00 × 10⁻² M) in acetone-d₆. The experimental (dots) and theoretical fitting (line) curves of ¹H NMR signals are shown right.

5.5.2 H4 ⊃ anthracene

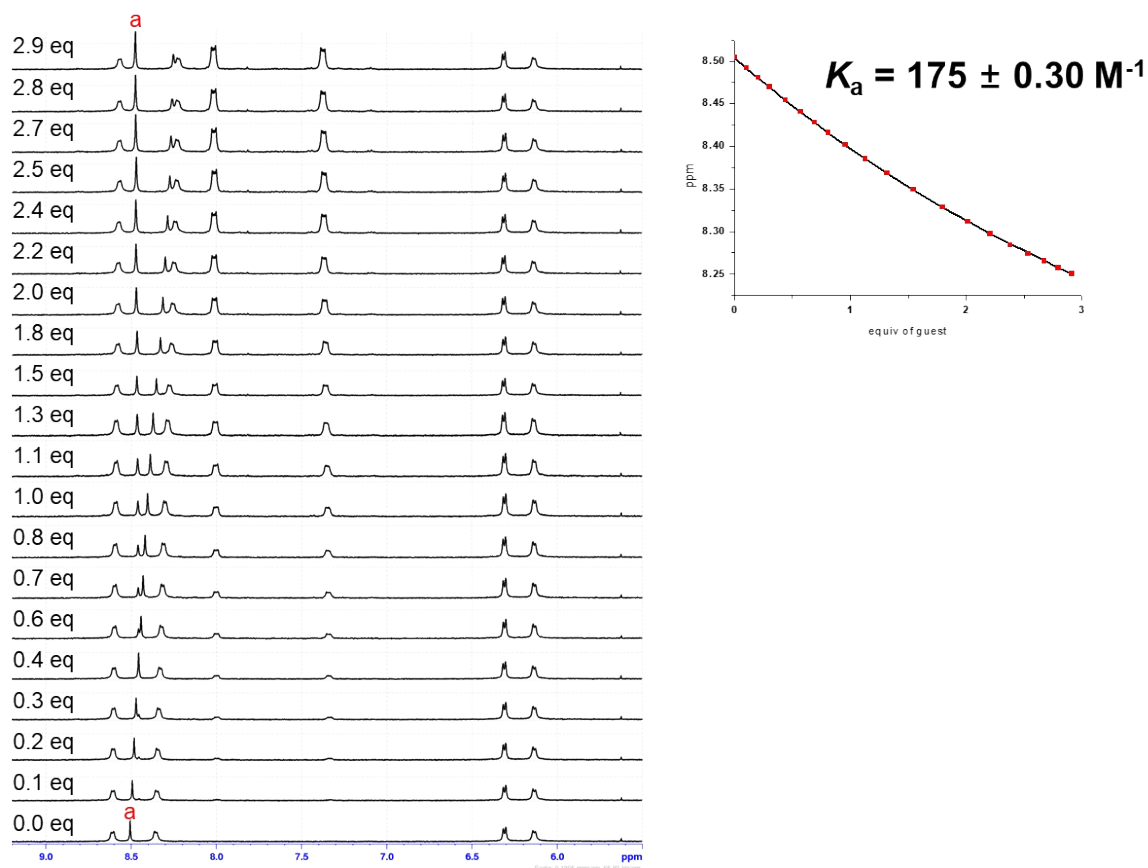


Figure S22. Partial ¹H NMR spectra of H4 (9.40 × 10⁻⁴ M) with the addition of anthracene (5.00 × 10⁻³ M) in acetone-*d*₆. The experimental (dots) and theoretical fitting (line) curves of ¹H NMR signals are shown right.

5.5.3 H4 ⊃ pyrene

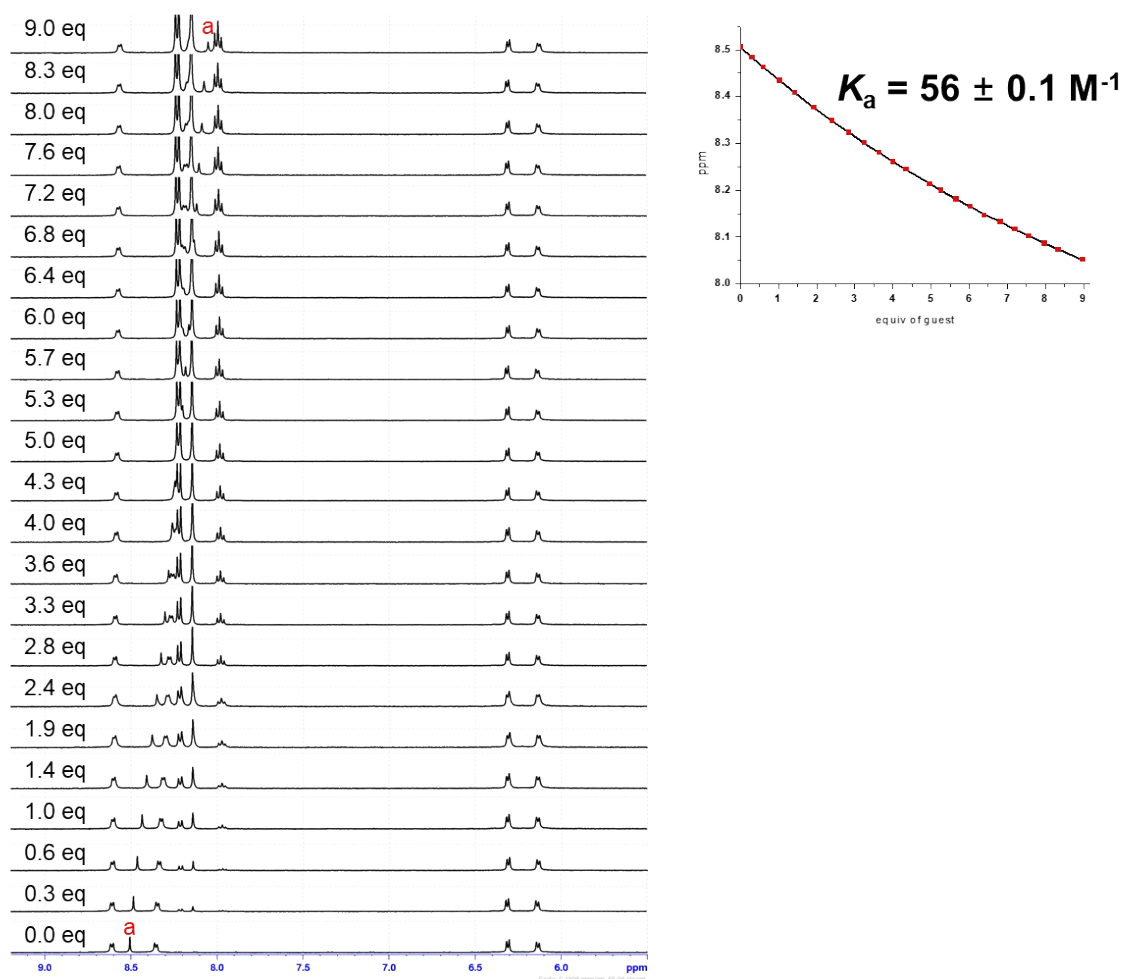


Figure S23. Partial ¹H NMR spectra of H4 (1.00 × 10⁻³ M) with the addition of pyrene (1.00 × 10⁻² M) in acetone-*d*₆. The experimental (dots) and theoretical fitting (line) curves of ¹H NMR signals are shown right.

5.5.4 H4 triphenylene

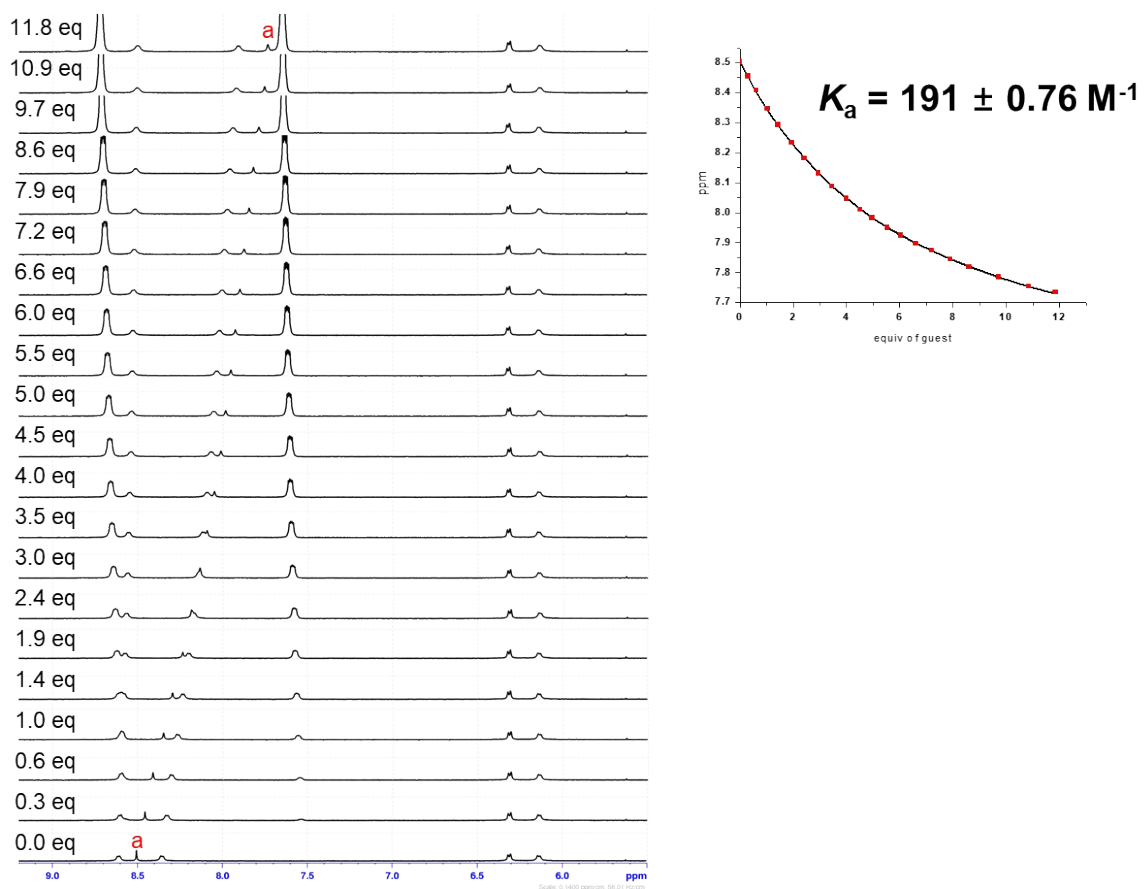


Figure S24. Partial ¹H NMR spectra of H4 (9.50 × 10⁻⁴ M) with the addition of triphenylene (1.50 × 10⁻² M) in acetone-d₆. The experimental (dots) and theoretical fitting (line) curves of ¹H NMR signals are shown right.

5.5.5 H4 ⊃ perylene

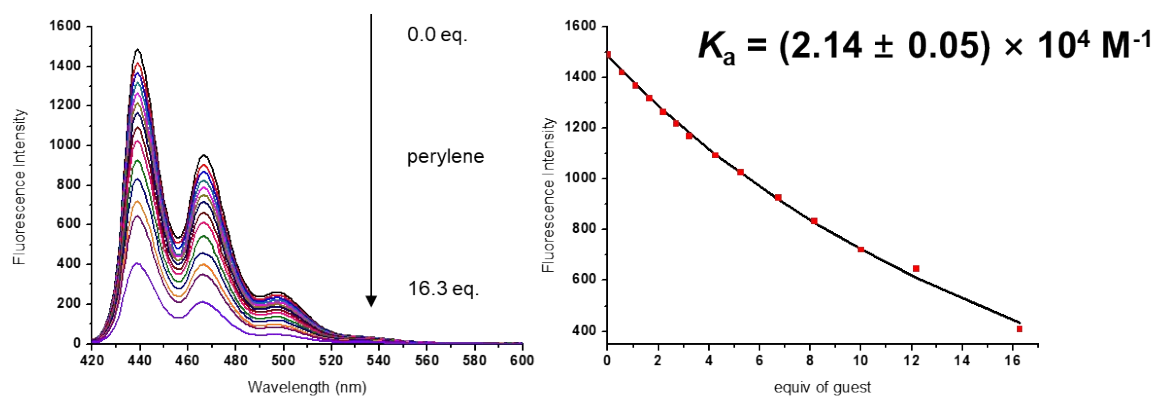


Figure S25. Fluorescence emission spectra (λ_{max} : 439 nm) of **H4** (2.00×10^{-6} M) with the addition of perylene in acetone, and fitting curve at 439 nm are shown right.

6. X-ray crystallographic analysis

6.1 Data Collection

The diffraction data from red crystals of **H2**⊃perylene (0.100 × 0.040 × 0.034 mm³) mounted on a MiTeGen MicroMount© were collected at 100 on a ADSC Quantum 210 CCD diffractometer with synchrotron radiation (0.630000 Å) at Supramolecular Crystallography 2D, Pohang Accelerator Laboratory (PAL), Pohang, Korea. The ADSC Q210 ADX program^{S7} was used for data collection (detector distance is 63 mm, omega scan; $\Delta\omega = 1^\circ$, exposure time is 1 sec/frame for **H2**⊃perylene and HKL3000sm (Ver. 703r)^{S8} was used for cell refinement, reduction and absorption correction.

6.2 Structure Solution and Refinement

The crystal structures of **H2**⊃perylene was solved by the direct method with SHELX-XT^{S9} and refined by full-matrix least-squares calculations with the SHELX-XL^{S10} in the Olex2^{S11} program package. The systematic absences in the diffraction data were uniquely consistent for triclinic, space group P-1 that yielded chemically reasonable and computationally stable results of refinement.^{S10,S11} A successful solution by the direct methods provided most non-hydrogen atoms from the *E*-map. The remaining non-hydrogen atoms were located in an alternating series of least-squares cycles and difference Fourier maps. All non-hydrogen atoms were refined with anisotropic displacement coefficients. All hydrogen atoms were included in the structure factor calculation at idealized positions and were allowed to ride on the neighboring atoms with relative isotropic displacement coefficients. The final least-squares refinement of 835 parameters against 15261 data resulted in residuals *R* (based on F^2 for $I \geq 2\sigma$) and *wR* (based on F^2 for all data) of 0.0613 and 0.1883, respectively. The final difference Fourier map was featureless.

To figure out the binding mode of hosts and guest, **H2**⊃perylene was determined by SC-XRD. However, in spite of our best efforts, other crystals, especially **H3** or **H4** containing the guests, were not obtained well.

Table 1 Crystal data and structure refinement for H2perylene.

Identification code	H2perylene
Empirical formula	C _{106.74} H _{97.64} Cl ₄ F _{13.48} N ₁₂ O _{22.85} Ru ₄ S ₄
Formula weight	2844.52
Temperature/K	100
Crystal system	triclinic
Space group	P-1
a/Å	10.352(2)
b/Å	14.444(3)
c/Å	19.699(4)
α/°	85.17(3)
β/°	79.84(3)
γ/°	72.63(3)
Volume/Å ³	2765.5(11)
Z	1
ρ _{calc} /g/cm ³	1.708
μ/mm ⁻¹	0.583
F(000)	1434.0
Crystal size/mm ³	0.1 × 0.04 × 0.034
Radiation	synchrotron (λ = 0.630)
2θ range for data collection/°	3.87 to 52
Index ranges	-14 ≤ h ≤ 14, -20 ≤ k ≤ 20, -27 ≤ l ≤ 27
Reflections collected	29921
Independent reflections	15261 [R _{int} = 0.0428, R _{sigma} = 0.0441]
Data/restraints/parameters	15261/114/835
Goodness-of-fit on F ²	1.056
Final R indexes [I ≥ 2σ (I)]	R ₁ = 0.0613, wR ₂ = 0.1837
Final R indexes [all data]	R ₁ = 0.0661, wR ₂ = 0.1883
Largest diff. peak/hole / e Å ⁻³	1.64/-1.54
CCDC number	2158142

7. Characterization data of new compounds, H3-H4

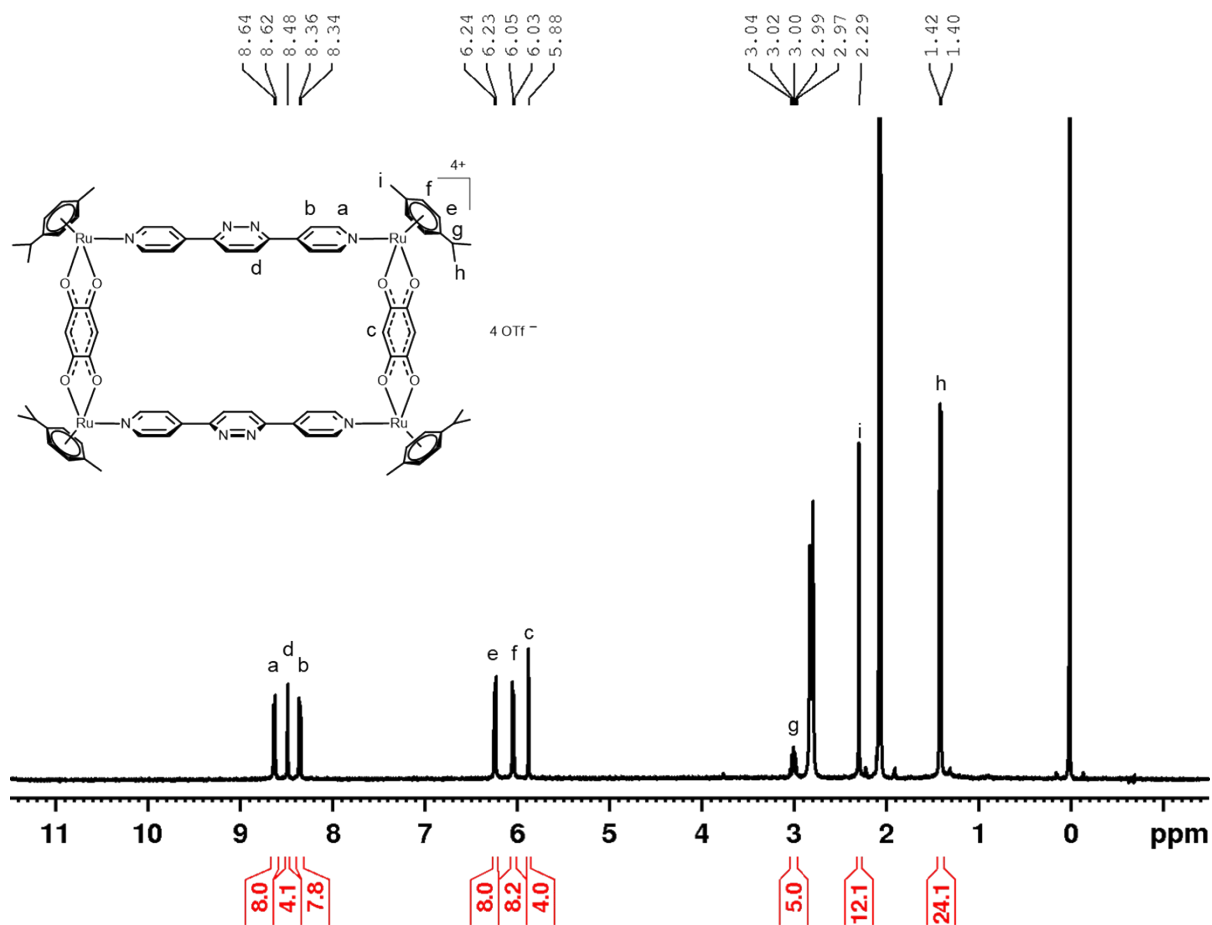


Figure S26. ^1H NMR of H3 (400 MHz, acetone- d_6 , 25 °C)

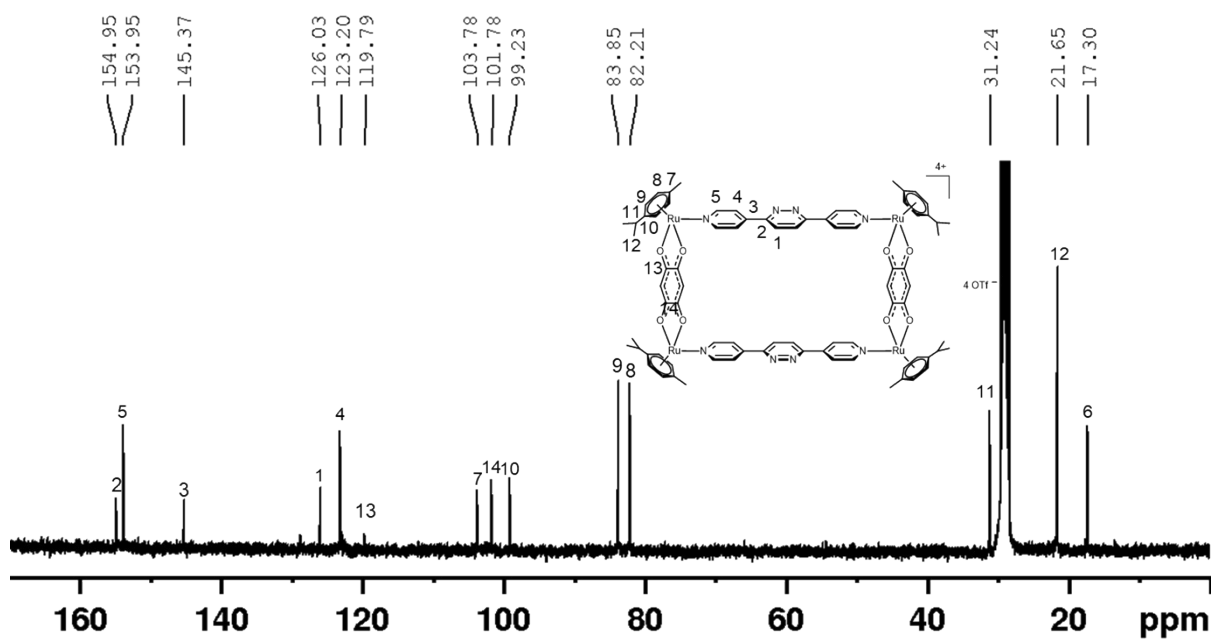


Figure S27. ^{13}C NMR of H3 (100 MHz, acetone- d_6 , 25 °C)

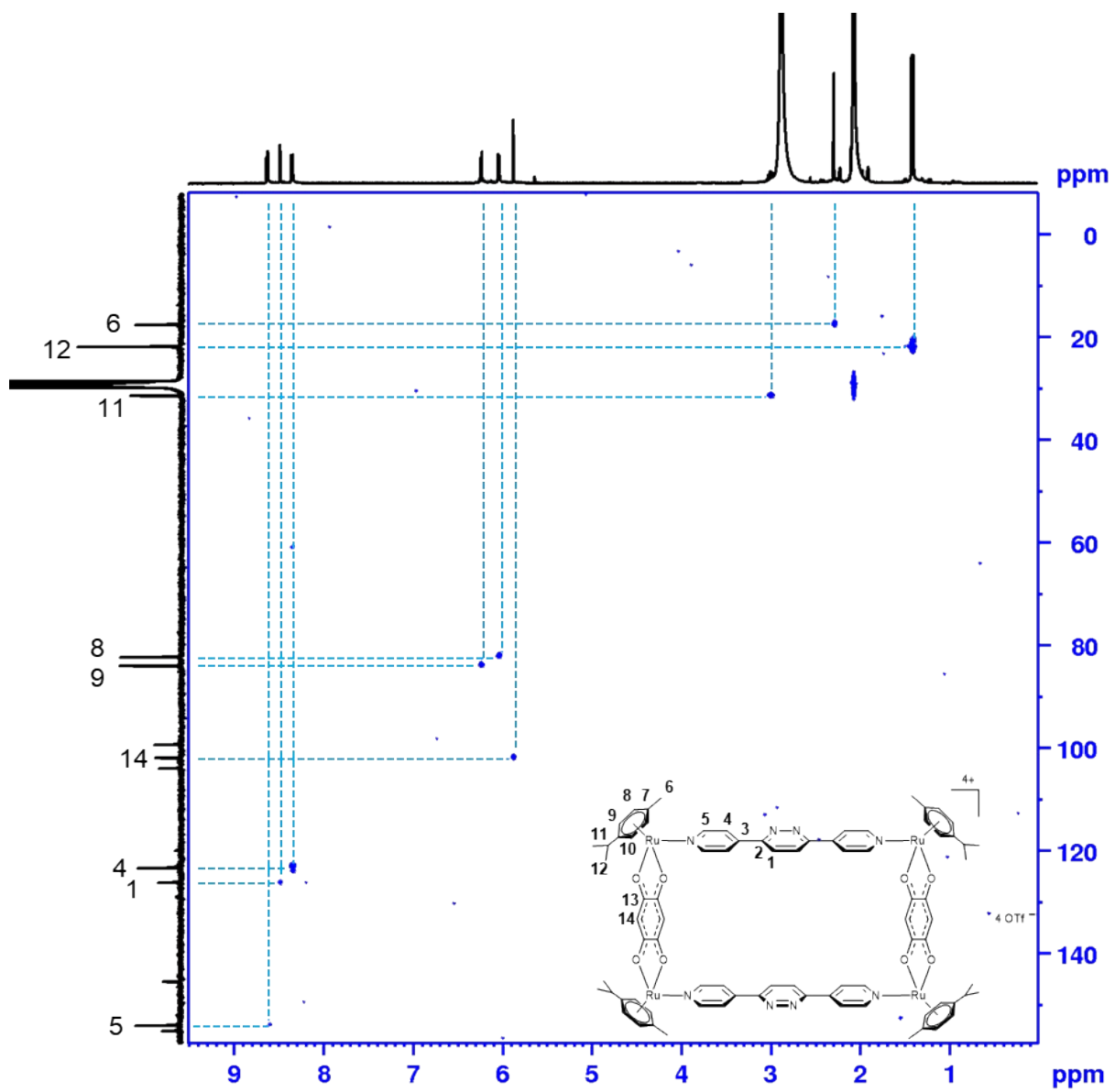


Figure S28. HSQC NMR of H3 (acetone- d_6 , 25 °C)

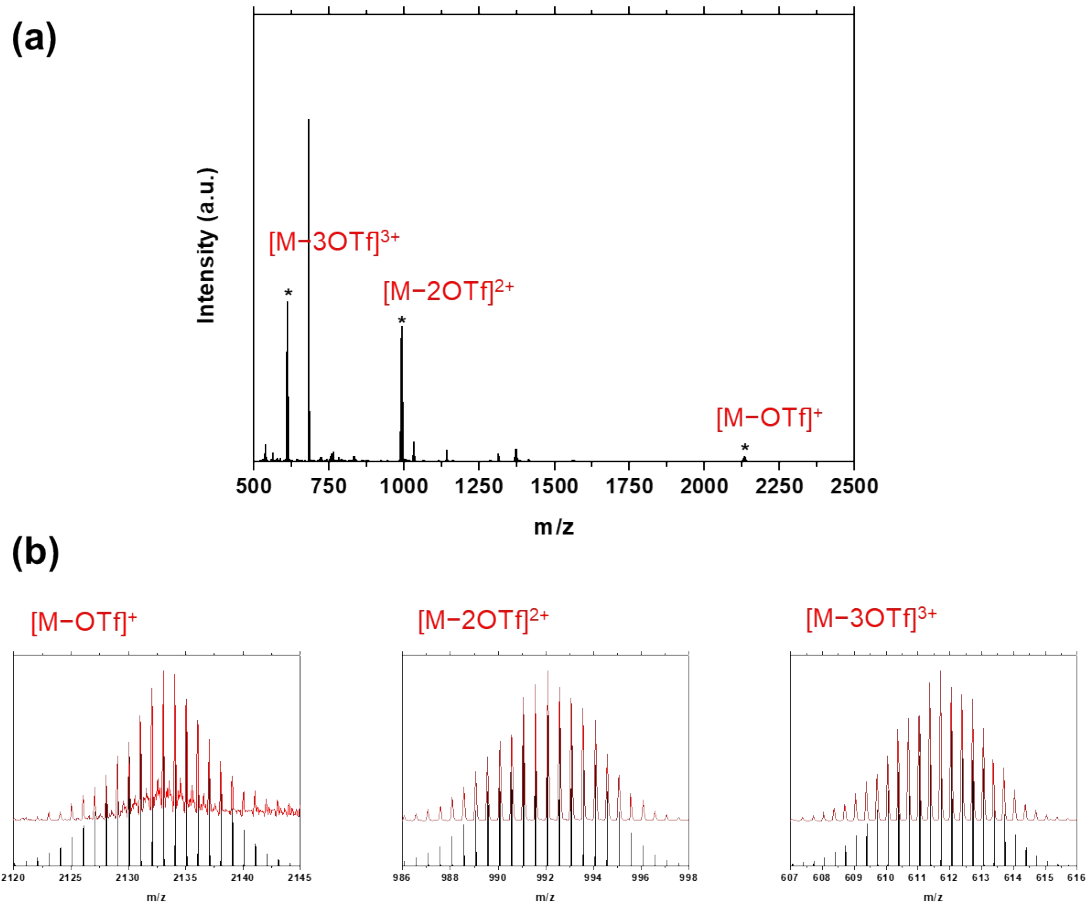


Figure S29. (a) ESI mass spectrum of the **H3**; (b) comparison of the experimental isotope pattern (red line) with the simulated isotope patterns (black line) of **H3**.

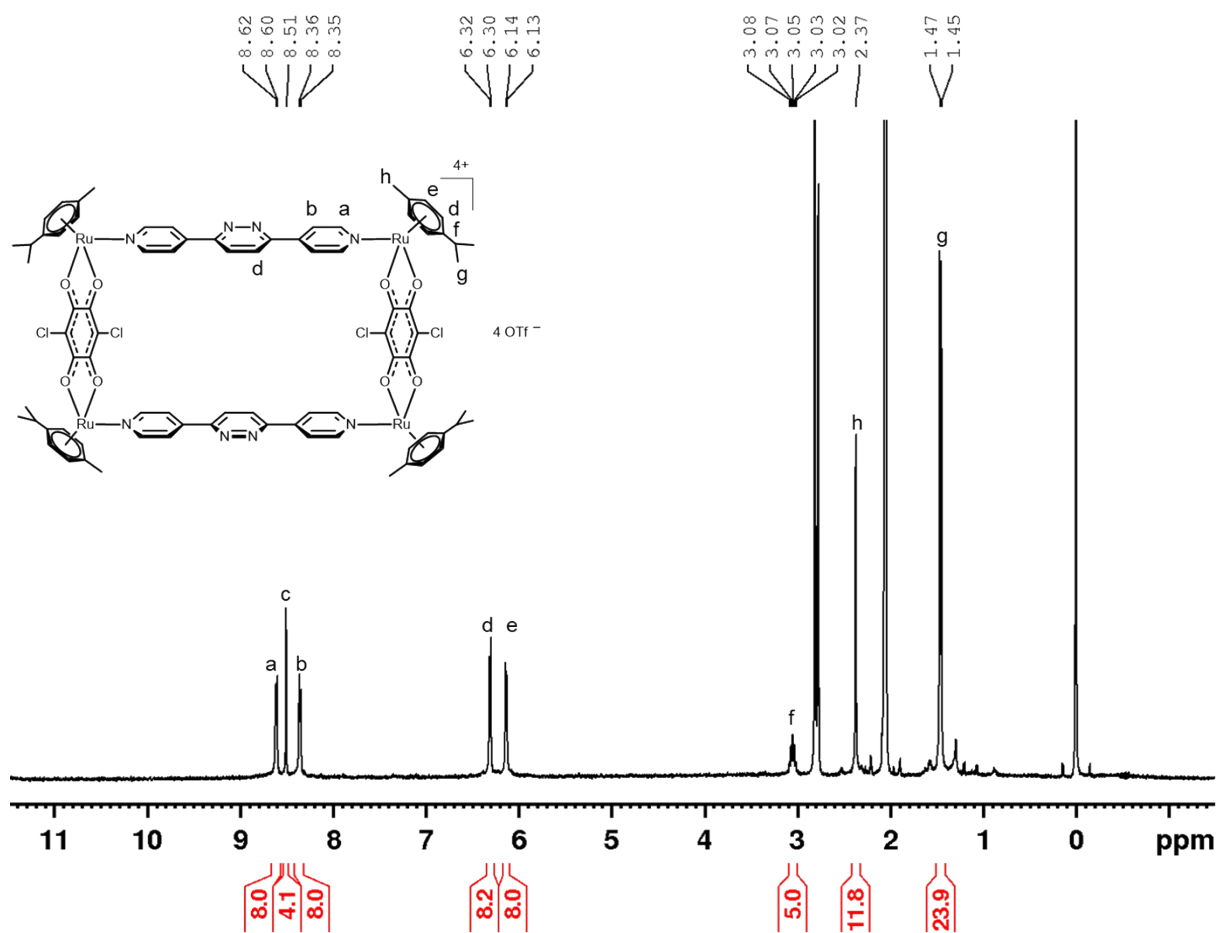


Figure S30. ¹H NMR of H4 (400 MHz, acetone-*d*₆, 25 °C)

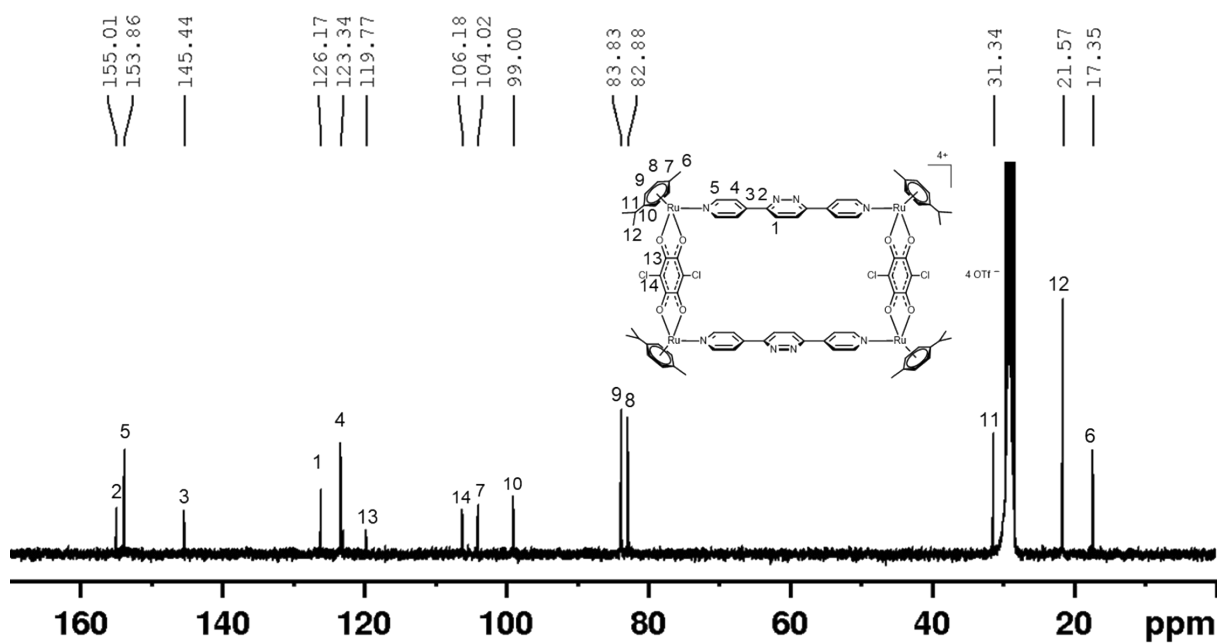


Figure S31. ¹³C NMR of H4 (100 MHz, acetone-*d*₆, 25 °C)

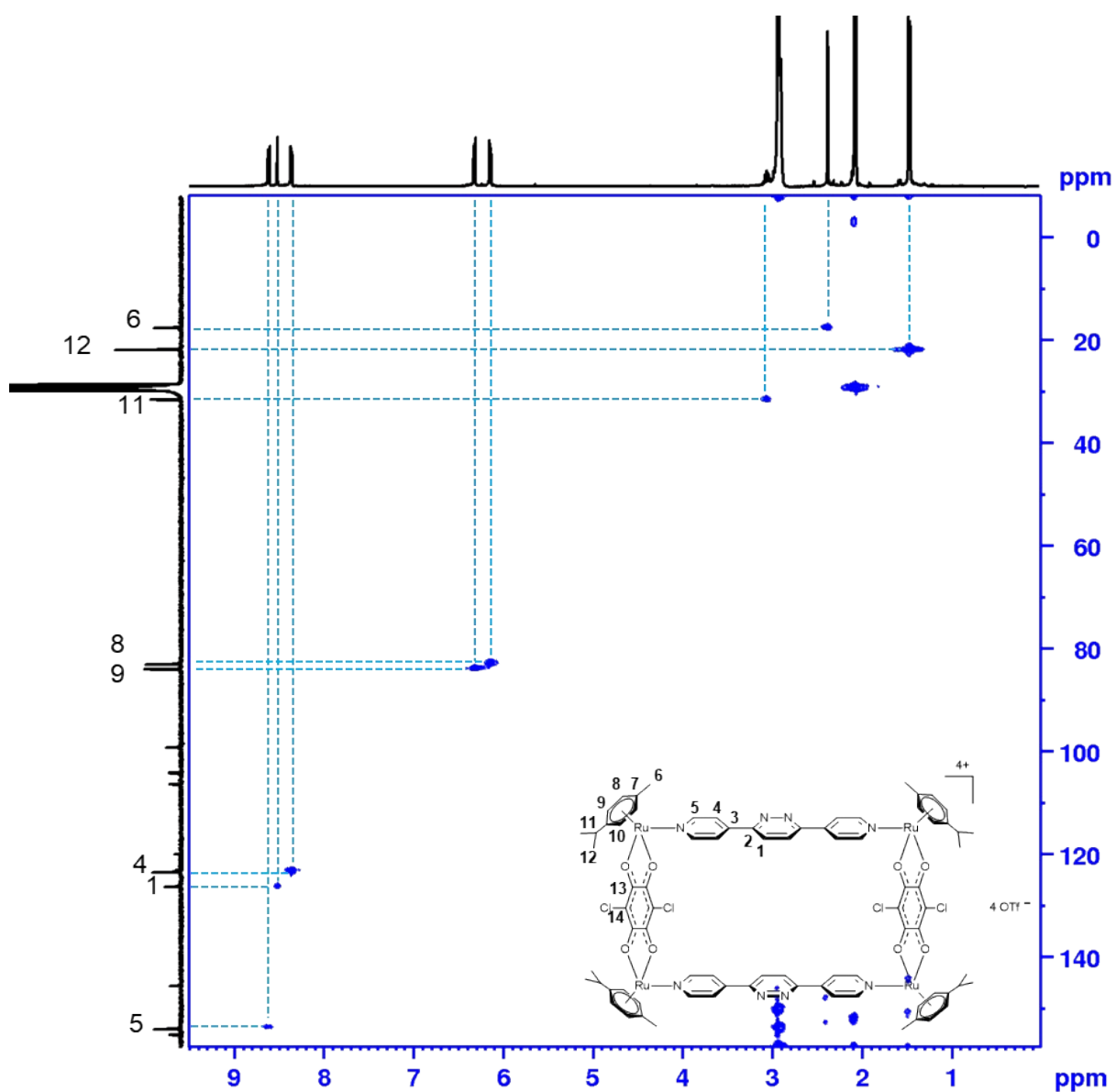


Figure S32. HSQC NMR of H4 (acetone- d_6 , 25 °C)

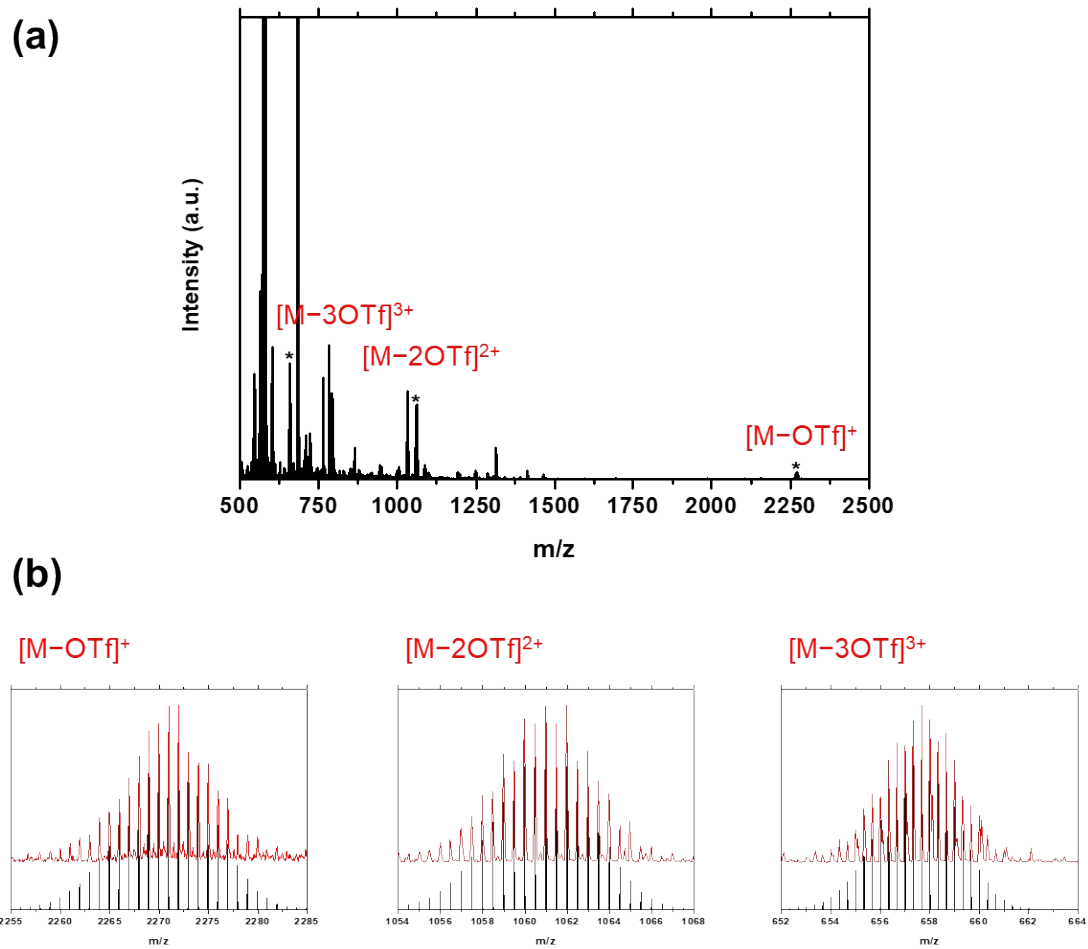


Figure S33. (a) ESI mass spectrum of the **H4**; (b) comparison of the experimental isotope pattern (red line) with the simulated isotope patterns (black line) of **H4**.

8. References

1. M. Fujita, M. Tominaga, A. Hori and B. Therrien, *Acc. Chem. Res.* 2005, **38**, 371–380.
2. J. Mattsson, P. Govindaswamy, J. Furrer; Y. Sei; K. Yamaguchi; G. Suss-Fink and B. Therrien, *Organometallics*, 2008, **27**, 4346–4356.
3. O. K. Farha, C. D. Malliakas, M. G. Kanatzidis and J. T. Hupp, *J. Am. Chem. Soc.* 2010, **132**, 950–952.
4. C. J. Hsu, S. W. Tang, J. S. Wang and W. Wang, *J. Mol. Cryst. Liq. Cryst.* 2006, **456**, 201–208.
5. E. Orhan, A. Garci and B. Therrien, *Inorganica Chim. Acta*, 2017, **461**, 78–83.
6. Bindfit www.supramolecular.org
7. A. J. Arvai and C. Nielsen, ADSC Quantum-210 ADX Program, Area Detector System Corporation: Poway, CA, USA, 1983.
8. Z. Otwinowski and W. Minor, *Methods in Enzymology*, 1997, **276**, 307–326.
9. G. M. Sheldrick, *Acta Cryst.* 2015, **A71**, 3–8.
10. G. M. Sheldrick, *Acta Cryst.* 2015, **C71**, 3–8.
11. O. V. Dolomanov, L. J. Bourhis, R. J. Gildea, J. A. K. Howard and H. Puschmann, *J. Appl. Crystallogr.*, 2009, **42**, 339–341.